



Contribution to “Diamond Jubilee of RCA”

Christoph E. Düllmann*, Michael Block, Fritz P. Heßberger, Jadambaa Khuyagbaatar, Birgit Kindler, Jens V. Kratz, Bettina Lommel, Gottfried Münzenberg, Valeria Pershina, Dennis Renisch, Matthias Schädel and Alexander Yakushev

Five decades of GSI superheavy element discoveries and chemical investigation

<https://doi.org/10.1515/ract-2022-0015>

Received January 20, 2022; accepted April 20, 2022;

published online May 16, 2022

Abstract: Superheavy element research has been a strong pillar of the research program at GSI Darmstadt since its foundation. Six new elements were discovered along with many new isotopes. Initial results on chemical properties of the heaviest elements were obtained that allowed for comparing their behavior with that of their lighter homologs and with theoretical predictions. Main achievements of the past five decades of superheavy element research at GSI are described along with an outlook into the future of superheavy element research in Darmstadt.

Keywords: GSI Darmstadt; SHIP; superheavy elements; TASCA; transactinides.

*Corresponding author: Christoph E. Düllmann, GSI

Helmholtzzentrum für Schwerionenforschung GmbH, Planckstr. 1, 64291 Darmstadt, Germany; Department Chemie – Standort TRIGA, Johannes Gutenberg-Universität Mainz, Fritz-Strassmann-Weg 2, 55128 Mainz, Germany; and Helmholtz-Institut Mainz, Staudingerweg 18, 55128 Mainz, Germany, E-mail: duellmann@uni-mainz.de

Michael Block, GSI Helmholtzzentrum für Schwerionenforschung GmbH, Planckstr. 1, 64291 Darmstadt, Germany; Department Chemie – Standort TRIGA, Johannes Gutenberg-Universität Mainz, Fritz-Strassmann-Weg 2, 55128 Mainz, Germany; and Helmholtz-Institut Mainz, Staudingerweg 18, 55128 Mainz, Germany

Fritz P. Heßberger, Jadambaa Khuyagbaatar, Birgit Kindler, Bettina Lommel, Valeria Pershina, Matthias Schädel and Alexander Yakushev, GSI Helmholtzzentrum für Schwerionenforschung GmbH, Planckstr. 1, 64291 Darmstadt, Germany

Jens V. Kratz, Department Chemie – Standort TRIGA, Johannes Gutenberg-Universität Mainz, Fritz-Strassmann-Weg 2, 55128 Mainz, Germany

Gottfried Münzenberg, GSI Helmholtzzentrum für Schwerionenforschung GmbH, Planckstr. 1, 64291 Darmstadt, Germany; and Institut für Physik, Johannes Gutenberg-Universität Mainz, Staudingerweg 7, 55128 Mainz, Germany

Dennis Renisch, Department Chemie – Standort TRIGA, Johannes Gutenberg-Universität Mainz, Fritz-Strassmann-Weg 2, 55128 Mainz, Germany; and Helmholtz-Institut Mainz, Staudingerweg 18, 55128 Mainz, Germany

1 Introduction

The laboratory synthesis of artificial elements heavier than uranium, the heaviest one found in large quantities on Earth, has started about 80 years ago, and the synthesis of the first transuranium element, ${}_{93}\text{Np}$, was reported in 1940 [1]. The race towards ever heavier elements is still ongoing, fueled by the quest for an “island of stability” of superheavy nuclei (SHN), the existence of which followed from calculations based on the shell model of atomic nuclei, e.g., [2]. These predicted that shell effects associated with the closure of the next nucleon shells beyond those at proton number $Z = 82$ and neutron number $N = 126$, giving rise to doubly magic ${}^{208}\text{Pb}$, would lead to increased fission barrier heights [3]. From about 1966 on, the next shell closures were generally expected at $Z = 114$ and $N = 184$ [2], and predictions appeared that suggested nuclei at and around the predicted doubly-magic nucleus ${}^{298}114$ to have half-lives that are longer than the age of the universe, cf., e.g., [4].

On the way towards exploring the limits of nuclear stability, the elements up to ${}_{100}\text{Fm}$ are accessible by neutron-capture reactions in research reactors [5]. Heavier ones can be produced in the laboratory in the collision of two nuclei. For this, projectile nuclei are accelerated to energies sufficiently high to overcome the Coulomb repulsion between the projectile and target nuclei, both of which are positively charged. Nuclear reaction products are separated by physical or chemical methods and are then analyzed for the presence of the desired heavy products. The progress of the synthesis of the heaviest elements has thus been intimately connected with the development of heavy ion accelerators and associated setups suitable for identifying the rare heavy reaction products, predominantly fusion products.

Germany entered the race towards the superheavy elements (SHE) – elements where all isotopes exist solely thanks to stabilizing nuclear shell effects – about five decades ago, with the proposed accelerator being a central component. Different competing proposals existed. Among them, the

UNiversal Linear ACcelerator (UNILAC), designed by Christoph Schmelzer, was chosen. Initially it was proposed to be built at Karlsruhe. The UNILAC was designed to allow acceleration of all elements up to ${}_{92}\text{U}$ to velocities sufficiently high to overcome the Coulomb barrier for any type of projectile/target combination. In April 1969, the decision was taken to found the Gesellschaft für Schwerionenforschung (GSI), and Darmstadt was selected as the location. The GSI was founded on December 17, 1969, with two partners; the Federal Republic of Germany and the State of Hessen. The name changed to GSI Helmholtzzentrum für Schwerionenforschung in 2008 to reflect GSI's role within the Helmholtz Association of German research centers. Historical aspects that led to the foundation of GSI have been described numerous times, see, e.g., references in [6].

Based on early predictions, cross sections of 100 mb were expected, leading to production rates of 10^6 s^{-1} . For the isolation of the produced superheavy nuclei, the Separator for Heavy Ion reaction Products (SHIP) [7] was designed and built and was ready for first experiments when first UNILAC-beams became available in 1976. At that time, discoveries of all elements up to ${}_{106}\text{Sg}$ were reported. Chemical approaches were developed as well to isolate new elements but also to study their chemical properties.

Over the course of 50 years since the construction of GSI, six new elements as well as many new nuclei were discovered at this location, see Figure 1.

Chemical studies initially focused on isolating long-lived isotopes from the complex nuclear reaction product mixture, before the focus shifted towards elucidating the chemical properties of the SHE. Figure 2 depicts the current Periodic Table of the Elements (PTE) with the SHE highlighted and with an emphasis on the elements studied at GSI. The SHE start a new series in the 7th row of the PTE. In the first ones, from ${}_{104}\text{Rf}$ to ${}_{112}\text{Cn}$, the 6d electron shell is being filled. After Cn, filling of the 7p shells occurs in the next six elements, from ${}_{113}\text{Nh}$ through ${}_{118}\text{Og}$. Heavier elements with $Z = 119$ and 120, waiting for their discovery, will belong to groups 1 and 2 of the PTE, accordingly, with the filling of the 8s shell. Since relativistic effects (RE) on the atomic orbitals (AOs) increase as Z^2 down the groups of chemical elements, it was predicted that their influence should be very strong in SHEs. The fundamental aspects of relativistic quantum theory and the influence of RE on chemical properties of SHEs are described in many publications, from pioneering works based on atomic relativistic calculations [9, 10], reaching today's sophisticated molecular and solid-state calculations [11]. According to these predictions, properties of the earlier transition metal elements (${}_{104}\text{Rf}$ through ${}_{108}\text{Hs}$), should be defined by the valence 6d AOs. Their gradual relativistic destabilization and expansion should result in the properties of SHEs being in line with the trends in the groups of chemical elements, however, with some peculiarities due to the large spin-orbit

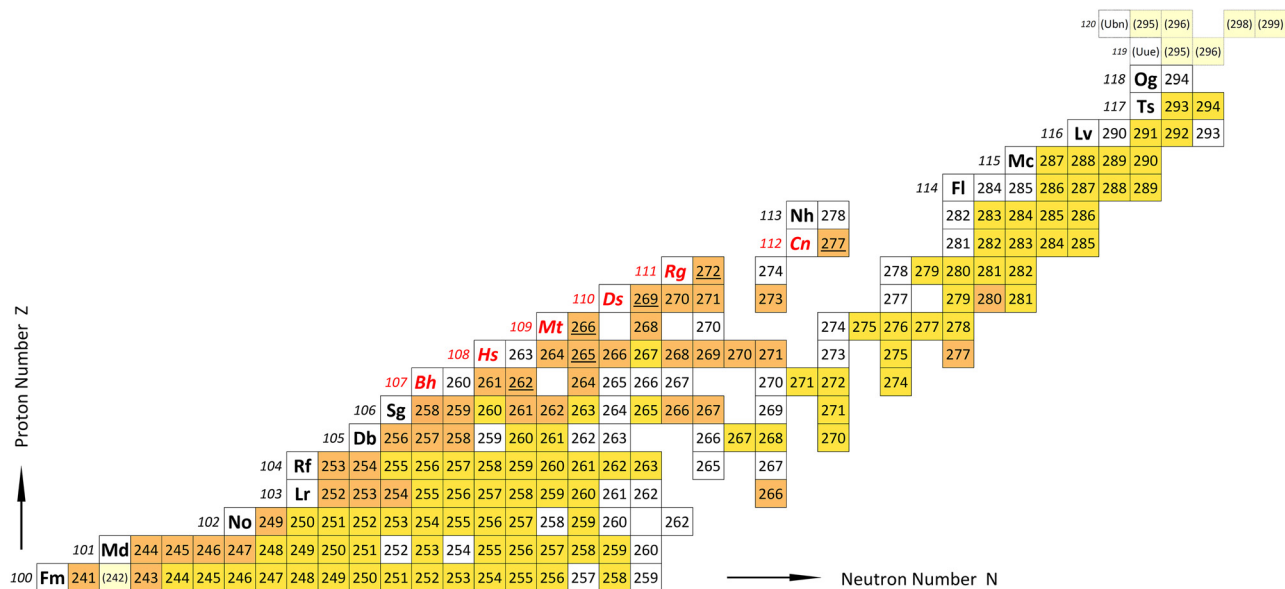


Figure 1: Chart of nuclei of the heaviest elements. For elements up to ${}_{118}\text{Og}$, known isotopes are shown. Nuclides discovered at GSI are indicated in orange boxes, and nuclides produced in experiments at GSI are indicated in yellow. Elements indicated with symbols in italics red have been discovered at GSI, with the underlined isotope being the discovery isotope. Isotopes of elements 119 and 120, which have been searched for but not discovered to date, are given with the mass number and element symbol in parentheses. The latter are based on the definition of IUPAC (International Union of Pure and Applied Chemistry) [8].

1																	18	
H																	He	
Li	Be											B	C	N	O	F	Ne	
Na	Mg	Al	Si	P	S	Cl	Ar											
K	Ca	Sc	Ti	V	Cr	Mn	Fe	Co	Ni	Cu	Zn	Ga	Ge	As	Se	Br	Kr	
Rb	Sr	Y	Zr	Nb	Mo	Tc	Ru	Rh	Pd	Ag	Cd	In	Sn	Sb	Te	I	Xe	
Cs	Ba	La-Lu	Hf	Ta	W	Re	Os	Ir	Pt	Au	Hg	Tl	Pb	Bi	Po	At	Rn	
Fr	Ra	Ac-Lr	Rf	Db	Sg	Bh	Hs	Mt	Ds	Rg	Cn	Nh	Fl	Mc	Lv	Ts	Og	
(Uue)	(Ubn)																	
Lanthanides		La	Ce	Pr	Nd	Pm	Sm	Eu	Gd	Tb	Dy	Ho	Er	Tm	Yb	Lu		
Actinides		Ac	Th	Pa	U	Np	Pu	Am	Cm	Bk	Cf	Es	Fm	Md	No	Lr		

Figure 2: Periodic table of the elements. Superheavy elements are shown in blue-bordered boxes. Elements discovered at GSI are marked by orange-filled boxes, and those confirmed at GSI before their official approval by yellow-filled boxes. Elements with symbols given in red have been chemically studied at GSI; in several cases, these were the first chemical studies of these elements. Elements 119 and 120 have not yet been discovered.

(SO) effects on the 6d-AOs. At the end of the d series, in groups 11 and 12, strong relativistic stabilization and contraction of the 7s AOs are predominant over the 6d AO's expansion and destabilization. This should result in an increase in inertness and stability of these elements, however, also in line with the trends in the groups. For even heavier, 7p elements, the influence of relativistic effects will be even more pronounced, particularly for ${}_{113}\text{Nh}$ and ${}_{114}\text{Fl}$, due to the stabilization and contraction of the $7p_{1/2}$ subshell and huge SO effects. Chemical studies conducted at GSI, both theoretical and experimental ones, therefore, had the ambitious goals to verify those trends and predictions, as well as to provide detailed information on the chemical behavior of SHEs.

In the past decades, the portfolio of topics studied in the heaviest elements has yet broadened. Optimizing and extending the synthesis of heaviest elements, mostly by fusion-evaporation but also by other reactions [12, 13], remains at the core of the program, not least as a prerequisite for any study of these nuclei and elements. Similarly, chemical studies form a second pillar [11, 14–16]. Also the study of the nuclear structure of heaviest elements, mainly by decay spectroscopy, remains as a pillar [17–19], but was extended by a program on high-precision direct mass measurements in the double-Penning-trap system

SHIPTRAP [20–22], where studies around the $N = 152$ neutron shell closure have been performed [23], employing the relatively high cross sections associated with the ${}^{48}\text{Ca} + \text{Pb}$ fusion reactions. More recently, laser spectroscopic studies of the heaviest elements were established [24], employing the Radiation Detected Resonance Ionization Spectroscopy (RADRIS) technique [25]. Again the region of Fm-No around the $N = 152$ neutron shell closure was in the focus of the first experiments, which contribute information on nuclear [26] as well as atomic [27] properties of the studied species. Comprehensive reviews, not limited to the work at GSI, are included in the 2015 special issue of “Nuclear Physics A” [28], which gives an overview of all relevant aspects of superheavy element research.

This article describes five decades of (SHE) studies at GSI, focusing on the experiments aimed at discovering new elements (Section 2) and at obtaining initial information about their chemical properties (Section 3). Besides the projectile beam provided by the heavy-ion accelerator, a stable layer of target nuclei able to withstand the intense beam is of prime importance for SHE synthesis. Targets of stable isotopes and the quasi-stable ${}^{238}\text{U}$ are produced in the GSI target laboratory, whereas targets of (highly) radioactive transuranium isotopes are prepared at the specialized infrastructure at the Department of Chemistry's TRIGA-Site

(the former Institute of Nuclear Chemistry) at Johannes Gutenberg University (JGU) Mainz (Section 4). The manuscript closes with an outlook into the next decade(s) of superheavy element research in Darmstadt.

2 Search for superheavy elements and discoveries

2.1 Early SHE searches and actinide

syntheses – reactions $^{238}\text{U} + ^{238}\text{U}$, $^{238}\text{U} + ^{248}\text{Cm}$ and $^{48}\text{Ca} + ^{248}\text{Cm}$

2.1.1 Transfer reaction studies with a ^{238}U beam on ^{238}U and ^{248}Cm targets

Driven by the quest for SHE [29], in a joint venture of the nuclear chemistry group at GSI and the JGU's Institute of Nuclear Chemistry, the experimental program with ^{238}U beams from GSI's UNILAC started in 1976 [16] with great optimism that a massive exchange of nucleons in so-called “damped collisions” would lead to the synthesis of SHE. All attempts to discover SHE in reactions of ^{238}U on ^{238}U remained unsuccessful [30–32]. Thereafter, in 1979, an international collaboration began an intense search for SHE in reactions of ^{238}U with ^{248}Cm targets. Again, no SHE were identified, pointing at cross sections being <40 pb for isotopes with half-lives between hours and several years [31, 32].

To explore the synthesis of heavy elements, ^{238}U targets were irradiated with 6.49–9.0 MeV/u ^{238}U beams. Applying liquid chromatography for chemical separation [33], cross sections were measured for actinide isotopes up to ^{256}Fm [34, 35]. This yielded isotope distributions, i.e., curves of cross sections versus mass number, for actinide elements up to ^{100}Fm . By exploiting the symmetry of the ^{92}U on ^{92}U reaction and making use of cross sections measured for complementary lighter elements, e.g., ^{84}Po for ^{100}Fm , details of the multi-nucleon transfer process were unraveled. Cross sections for the surviving heavy actinides indicate that they are produced in the low-energy tails of the dissipated energy distributions, however, with a low-energy cutoff at ≈ 35 MeV. Excitation functions show that identical isotope distributions are populated independent of the bombarding energy, indicating that the same bins of excitation energy are responsible for the production of these fissile isotopes. This provided a better understanding of the synthesis of heavy actinides and transactinides in transfer reactions [35, 36], elucidated limitations (dynamical hindrance), and challenged diffusion model calculations [37].

A big step forward in the production of heavy elements and deeper insights into the synthesis mechanism came from studies of ^{238}U on ^{248}Cm performed at GSI in collaboration with US national laboratories [35, 38]. Again, chemical separations were performed [16, 33]. The enhancement of the formation of transcurium isotopes in the reaction of ^{238}U on ^{248}Cm is shown in Figure 3. Cross sections for ^{100}Fm , ^{99}Es , and ^{98}Cf are three to four orders of magnitude higher than in the ^{238}U on ^{238}U reactions [35, 38]. Evaporation calculations assign the surviving heavy actinides to $3n$ and/or $4n$ evaporation channels from primary fragments. Together with data from the ^{238}U on ^{238}U reaction, the results from the ^{238}U on ^{248}Cm reaction provided anchor points that still serve as benchmarks for theoretical calculations and extrapolations [39, 40].

2.1.2 The $^{48}\text{Ca} + ^{248}\text{Cm}$ reaction

With a completely different outcome, heavy and superheavy element programs based on reactions of ^{48}Ca on ^{248}Cm were performed at GSI in two periods: a first one in 1982–1983, following up on experiments previously performed in Dubna, Russia, and in Berkeley, USA; see [32] for

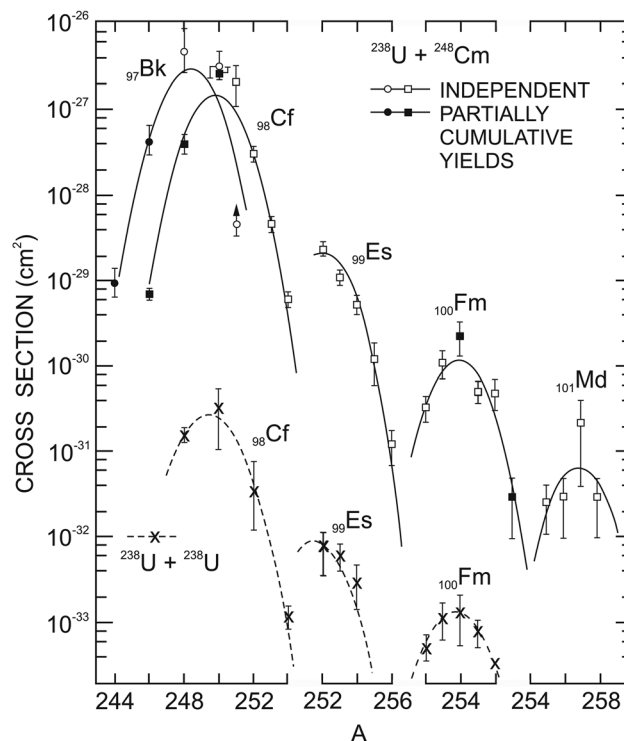


Figure 3: Cross sections for the formation of target-like transcurium isotopes in the $^{238}\text{U} + ^{248}\text{Cm}$ reaction at ≤ 7.40 MeV/u in comparison with data for the $^{238}\text{U} + ^{238}\text{U}$ reaction at ≤ 7.50 MeV/u; see [35] for more details. (Reprinted figure with permission from J.V. Kratz et al., Phys. Rev. C 88, 054,615 (2013), <https://doi.org/10.1103/PhysRevC.88.054615>. © 2013 by the American Physical Society).

a status report of all SHE searches up to that time. A more recent program began in 2005.

At first, in a collaborative effort, groups from the GSI, the JGU, and the Lawrence Berkeley National Laboratory (LBNL) as the leading partners, carried out experiments not only applying the Small Angle Separating SYstem (SASSY) at LBNL's SuperHILAC accelerator and SHIP at the UNILAC but also a variety of chemical separations. Due to insufficient sensitivity in this early period, SHE were not discovered [41]; see Figure 4.

However, deeper insights into the synthesis of heavy elements in multi-nucleon transfer reactions were gained from cross section measurements of heavy actinide isotopes and their complementary below-target elements [42].

In 1982–1983, SHE fractions were chemically separated manually at the LBNL. Thereafter, at the GSI, a new level of sophistication was reached by a continuous transport of nuclear reaction products with He/KCl-cluster jets to gas-phase chemistry devices and, as an essential step in liquid-phase chemistry [14, 16], to the first version of the Automated Rapid Chemistry Apparatus (ARCA) [43]. It drastically speeded up transport and separation times giving access to nuclides with half-lives in the range of minutes. In these experiments, cross section limits for SHE were obtained in the 0.1 nb range for nuclides with half-

lives from minutes to hours [41]; see curves 3, 4, and 5 in Figure 4 and [16, 42] for experimental details.

At various bombarding energies of ^{40}Ca and ^{48}Ca ions on ^{248}Cm targets, isotope cross sections of $_{86}\text{Rn}$ through $_{92}\text{U}$ (below-target elements) and $_{97}\text{Bk}$ through $_{100}\text{Fm}$ (above-target elements) were obtained in radiochemical experiments performed at LBNL and GSI. The following insights into the synthesis of above-target element isotopes were derived from these experiments [42, 44]: (i) The maxima of the isotope distributions are located at only 2–3 mass numbers larger for ^{48}Ca than for ^{40}Ca reactions. (ii) Shapes and half-widths of these distributions are similar to those observed earlier for reactions with lighter-element projectiles and the widths are smaller than the ones obtained from ^{238}U -induced reactions [38]. (iii) While the excitation functions for ^{40}Ca peak near the Coulomb barrier, those for ^{48}Ca peak at ≈ 20 MeV above the barrier. (iv) In reactions with ^{48}Ca , isotopes are produced essentially cold, i.e., with very low excitation energy of $\approx (0\text{--}12)$ MeV for $_{99}\text{Es}$ and $_{100}\text{Fm}$.

After successfully using ARCA in ^{48}Ca on ^{248}Cm experiments, improved versions of ARCA were applied. The unique potential of ^{254}Es targets was probed in searches for SHE [45, 46] and the synthesis of the most neutron-rich isotopes of the heaviest actinides [47]. ^{136}Xe on ^{244}Pu experiments led to the discovery of ^{243}Np and ^{244}Np [48] and confirmed the outstanding role of ^{136}Xe as a projectile to maximize the production of below-target neutron-rich nuclides in transfer reactions.

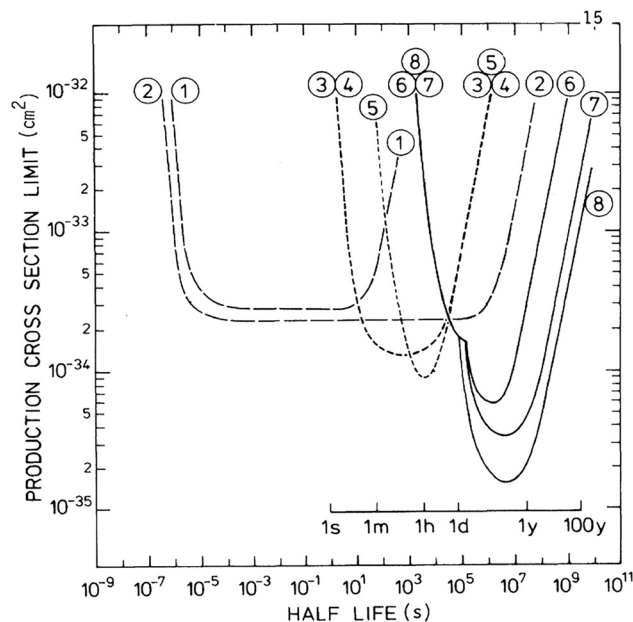


Figure 4: Upper limit cross sections for SHE production in the ^{48}Ca on ^{248}Cm reaction in the energy range of 4.5–5.2 MeV/u as a function of the half-life. Data are results from recoil separators (curves 1 and 2) and from a variety of chemical methods (3–8); see [41] for details. (Reprinted figure with permission from P. Armbruster et al., Phys. Rev. Lett. 54, 406–409 (1985), <https://doi.org/10.1103/PhysRevLett.54.406>. © 1985 by the American Physical Society).

2.2 Fusion-evaporation reactions at recoil separators – SHE searches and discoveries

The probability to form SHN in fusion-evaporation reactions is extremely low; state-of-the-art experimental separation and detection techniques are required for successful experiments [49]. A dedicated instrument, the SHIP, has been built in the mid-1970s [7]. SHIP is a two-stage velocity filter with separated electric and magnetic fields (Figure 5a), which efficiently separates evaporation residues (ER) from other ions recoiling from the target, because of their significantly different kinematics [7]. ER are implanted into a position-sensitive silicon detector to measure their radioactive decay [50]. Decays of the ER and their daughter nuclei can be correlated, allowing identification of new isotopes and even new elements based on one single measured α -decay sequence [51].

At SHIP, the elements with $Z = 107$ to $Z = 112$, bohrium ($_{107}\text{Bh}$), hassium ($_{108}\text{Hs}$), meitnerium ($_{109}\text{Mt}$), darmstadtium

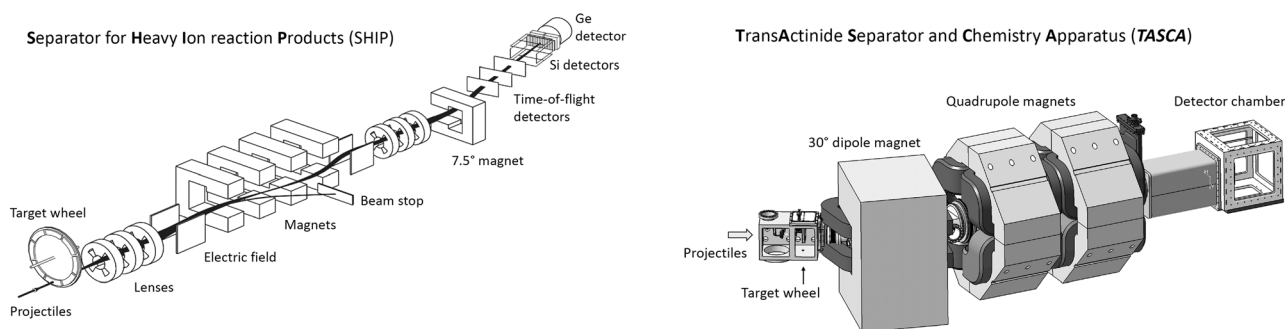


Figure 5: The two recoil separators installed at GSI. Left: SHIP [7] in its upgraded version [49], total length 13 m, flight time of recoils 2 μ s. Right: Schematic drawing of TASCA [55], total length 3.5 m, flight time of recoils 0.6 μ s. (Left panel: Reprinted figure with permission from S. Hofmann et al., *Rev. Mod. Phys.* 72, 733–767 (2000), <https://doi.org/10.1103/RevModPhys.72.733>. © 2000 by the American Physical Society).

($_{110}\text{Ds}$), roentgenium ($_{111}\text{Rg}$), and copernicium ($_{112}\text{Cn}$) were discovered using cold fusion-evaporation reactions using doubly magic ^{208}Pb or its neighbor ^{209}Bi as targets, irradiated by ^{54}Cr , ^{58}Fe , $^{62,64}\text{Ni}$, and ^{70}Zn beams [49].

The discovery of $_{108}\text{Hs}$ proofed the concept of SHEs, the existence of nuclei solely by shell stabilization [3, 52]. The discovery of the region of shell-stabilized hexadecapole-deformed nuclei centered at $Z = 108$ and $N = 162$ [53, 54] paved the way towards the present top of the chart of nuclei.

In the late 2000s, the gas-filled TransActinide Separator and Chemistry Apparatus (TASCA), see Figure 5b, was put into operation [55]. Its magnets came from a post-separator used behind SHIP in the late 1980s and early 1990s [56]. The TASCA is very efficient for the collection of SHN while background suppression is not as high as in SHIP. Application of the correlation method under larger background is possible thanks to double-sided silicon-strip detectors, which provide thousands of pixels for determining the positions of implanted nuclei. Fast digital electronics allows resolving radioactive decays occurring on sub- μ s timescales [57]. When TASCA became available for the search for new SHE, the elements with $Z = 113$ –118 had already been claimed to be discovered at the Gas-filled Recoil Ion Separator (GARIS), operating at RIKEN, Wako-shi, Japan ($Z = 113$) [58], and at the Dubna Gas-Filled Recoil Separator (DGFRS) at the Flerov Laboratory for Nuclear Reactions (FLNR), Dubna (Russia) ($Z = 114$ –118) [59]. Accordingly, the new element synthesis program at TASCA was dedicated to searches for elements $Z = 119$ and 120.

2.2.1 New SHE from SHIP

2.2.1.1 The first series: bohrium, hassium, and meitnerium

The SHE program at SHIP started with element 105, now named dubnium, and proceeded stepwise towards heavier SHE. As the method was new, the first experiments to create new elements were carried out as companion

experiments; e.g., prior to element 107 synthesis, isotopes of the α -decay daughter Db were produced to test the experimental method and to create a safe basis for the parent-daughter correlation by studying the decay properties of the expected daughter isotopes.

Element 107, later named bohrium, was the first element discovered at SHIP, based on observed six atoms from the $^{54}\text{Cr} + ^{209}\text{Bi}$ reaction in February 1981 [51]. Figure 6 displays one of these α -decay chains from an implanted nucleus, together with two selected daughter chains from the companion experiment. The lifetimes of individual nuclei show (expected) statistical fluctuations. As the range of α particles in silicon is larger than the implantation depth of the nuclei, only about half of the α particles are registered with full energy in the stop detector, leading to partly incomplete chains. The chains end in known α decays of ^{250}Fm , and ^{250}Md and, thus, could be assigned to ^{258}Db and ^{262}Bh . These results were confirmed later [60].

Next, element 109, meitnerium, was discovered in 1982 in the reaction $^{209}\text{Bi}(^{58}\text{Fe},n)^{266}\text{Mt}$ [51] via a single decay sequence observed in a 19-day long experiment [61]. A nuclear-chemical study at FLNR [62] measured the long-lived ^{266}Mt progeny ^{246}Cf , supporting the assignment, which was later also confirmed in further experiments at SHIP in 1988 [63] and 1997 [64]. In the latter, 12 additional ^{266}Mt atoms were observed. The nuclide features α -decay energies in the wide range of 10.5–11.8 MeV; this is a common feature of odd–odd SHN.

Element 108, hassium, was discovered in 1984 in the reaction $^{208}\text{Pb}(^{58}\text{Fe},n)^{265}\text{Hs}$ [65] based on three decay chains. The assignment was supported by a $^{208}\text{Pb}(^{54}\text{Cr},xn)$ companion experiment to produce $^{259-261}\text{Sg}$. In 1986, even–even ^{264}Hs was observed in the $^{58}\text{Fe} + ^{207}\text{Pb}$ reaction [49]. The Hs experiments were performed after the Mt one. Theory predicted spontaneous fission half-lives below microseconds for even–even Hs isotopes [66]. Mt, via odd–odd ^{266}Mt , was synthesized first. This was expected to have a long partial fission half-life

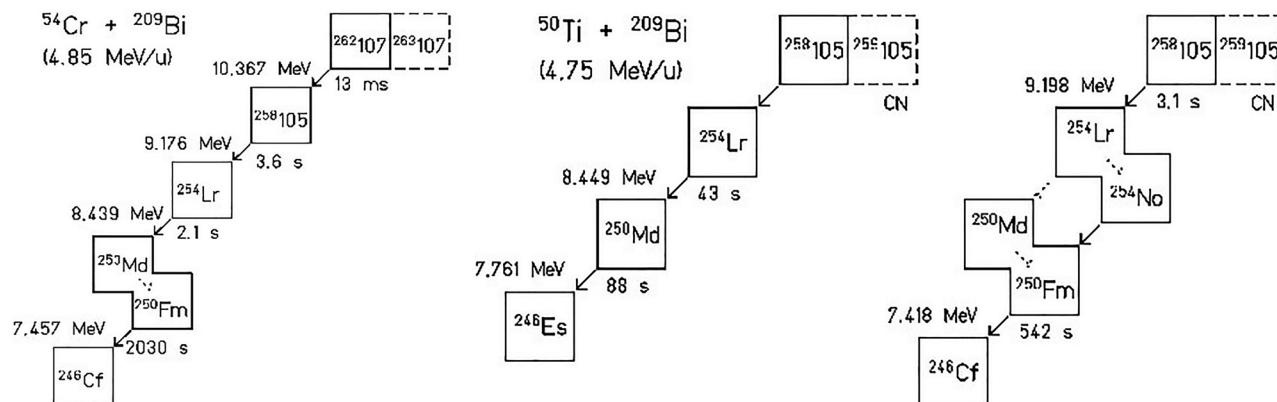


Figure 6: Left panel: A single-atom decay chain ending in the decay of ^{250}Fm . Right panel: two examples of daughter chains. (Reprinted by permission from Springer-Verlag Zeitschrift für Physik A, Identification of Element 107 by α correlation chains, G. Münzenberg et al. Z. Phys. A 300, 107–108 (1981), © 1981).

due to an unpaired proton and an unpaired neutron, thus, profiting twice from fission hindrance of unpaired nucleons. This was expected to enhance the fission half-life by about 10^6 -fold. The unexpected observation of α decay for Hs, especially for even–even ^{264}Hs , together with the results for even–even ^{260}Sg , was a first hint at a region of enhanced shell stabilization of nuclei centered at $Z = 108$ and $N = 162$ [54]. This was later confirmed and the nucleus located at the center of this region, ^{270}Hs , was discovered in 2006 in Hs chemistry experiments [67] (Section 3.2).

2.2.1.2 The second series: darmstadtium, roentgenium, and copernicium

Although the elements with $Z = 107$ – 109 were discovered in the 1980s, shortcomings of the experimental method and set-up became evident: (a) quite low beam intensities of ≈ 100 – $200 \text{ nA}_{\text{part}}$ ($1 \text{ nA}_{\text{part}} = 6.24 \cdot 10^9 \text{ s}^{-1}$), (b) small transmission of SHIP of $<30\%$ for the considered reactions, (c) limitations in the detection efficiency of the detector system, and (d) insufficient knowledge of the production mechanism. These limited proceeding to heavier elements accessible at expectedly lower rates but were overcome within a few years. A high-charge-state injector consisting of an radiofrequency quadrupole (RFQ) + interdigital H-mode (IH) acceleration structure equipped with an electron-cyclotron resonance (ECR) ion source provided beam intensities $>500 \text{ nA}_{\text{part}}$ [68]. The target position was shifted closer to the SHIP entrance, increasing the transmission by about two-fold [69]. The old ‘stop’ detector comprising seven individual detectors was replaced by a single 16-strip detector. A box of silicon detectors was mounted, surrounding the backward hemisphere of the stop detector to measure escaping α particles [68]. Excitation functions of the $^{208}\text{Pb}(^{50}\text{Ti},1-2n)^{256,257}\text{Rf}$ [70] and $^{208}\text{Pb}(^{58}\text{Fe},n)^{265}\text{Hs}$ [64] reactions were measured to improve

the understanding of the cold-fusion reaction mechanism, guiding the selection of optimum bombarding energies for producing heavier nuclei.

The synthesis of new elements was resumed in November 1994. The $^{269}110$ was the first isotope of element 110, later named darmstadtium. Within 13 days, three atoms were observed in the $^{62}\text{Ni} + ^{208}\text{Pb}$ reaction [68]. Then, the beam was switched to ^{64}Ni to produce ^{271}Ds [71]. The cross-section increased ≈ 6 -fold compared to ^{269}Ds ; thus, the search for element 111, roentgenium, was started using the reaction $^{209}\text{Bi}(^{64}\text{Ni},n)^{272}\text{Rg}$. In 18 days three decay events of ^{272}Rg were registered in December 1994 [72]. In January 1996, an attempt to produce element 112, copernicium, in the reaction $^{70}\text{Zn}(^{208}\text{Pb},n)^{277}\text{Cn}$ started. After 34 days of irradiation, two decays attributed to ^{277}Cn were published [73]. A reanalysis of the data performed five years later revealed that the first decay chain had been created spuriously. However, in a follow-up experiment, a second real ^{277}Cn decay chain had been observed [74].

2.2.2 Search for new elements 119 and 120 at SHIP and TASCA

After the discoveries of the elements $_{107}\text{Bh}$ to $_{112}\text{Cn}$ [49] it became obvious that cold fusion-evaporation reactions will result in extremely low cross sections for the synthesis of yet heavier elements. This was since proven by the discovery of element 113 at GARIS, see Figure 7. About 550 days of beam time yielded the observation of three atoms [58]. However, shell-stabilized nuclei can also be used in projectile-target combinations for SHE synthesis in hot-fusion reactions based on the doubly-magic ^{48}Ca projectile and actinide targets. Such reactions had already been considered for SHE synthesis in the 1970–1980s (see

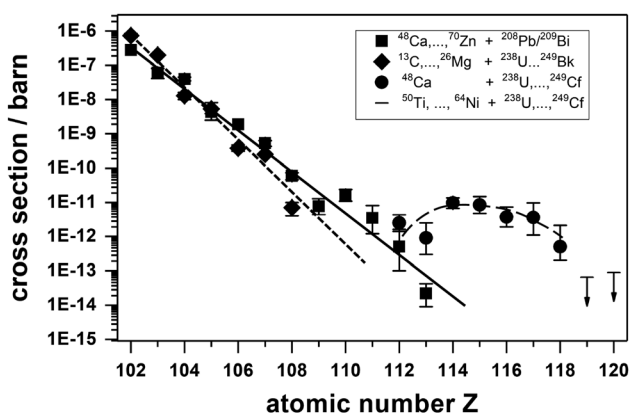


Figure 7: Experimentally measured maximum cross sections for the production of elements with $Z = 102$ – 118 as well as lowest reported upper limits for elements with $Z = 119$ and 120 . The fits (solid: Cold fusion reactions; short-dashed: Hot-fusion reactions with light projectiles; long-dashed: ^{48}Ca -induced reactions) are shown to guide the eye.

Section 2.1.2), albeit unsuccessfully. The sensitivity for such experiments had since been significantly improved at the DGFRS in the late 1990s. As a result, the elements 114 – 118 were discovered at FLNR [59].

In 2006, ^{48}Ca -beam based campaigns restarted at GSI. First, ^{283}Cn , which has six neutrons more than the ^{277}Cn produced by cold fusion, was synthesized via the $^{48}\text{Ca} + ^{238}\text{U}$ reaction at SHIP [75]. The permission to irradiate transuranium targets at SHIP and at TASCA enabled the synthesis and study of ^{114}Fl [76], ^{115}Mc [77] and ^{117}Ts [78] at TASCA and of ^{116}Lv at SHIP [79].

The continuation of the synthesis of SHE beyond ^{118}Og faces many experimental challenges. Fusion-evaporation reactions with projectiles beyond ^{48}Ca have to be used, due to insufficient amounts of isotopes with $Z > 98$ to make targets [5].

2.2.2.1 Search for element 120

Four reactions, $^{64}\text{Ni} + ^{238}\text{U}$, $^{58}\text{Fe} + ^{244}\text{Pu}$ [80], $^{54}\text{Cr} + ^{248}\text{Cm}$, and $^{50}\text{Ti} + ^{249}\text{Cf}$ are considered to synthesize element $Z = 120$. Its discovery was attempted in three of them at GSI. Theories predicting the next proton shell closure to occur at $Z = 114$ predict microsecond-half-lives for the $Z = 120$ isotopes produced in these reactions. This should still be long enough to survive the flight through compact recoil separators, but detection requires a fast data-acquisition system, prompting an essential upgrade for the focal plane detection technique. To this end, a fast digital data acquisition system was implemented prior to search for element 120 [57].

In 2007, SHIP was not yet approved for irradiations of highly radioactive targets, so the reaction $^{64}\text{Ni} + ^{238}\text{U}$ was chosen for a first attempt, although the predicted cross section was only ≈ 5 fb [39]. As such theoretical predictions are rather uncertain, the actual cross-section was hoped to

be considerably higher. In experiments performed in 2007/08, a cross-section limit of ≈ 90 fb was reached [81]. No decay chain was observed that could be attributed to a $Z = 120$ isotope. In spring 2012, another attempt was undertaken at SHIP, using the $^{54}\text{Cr} + ^{248}\text{Cm}$ reaction. In a ≈ 40 -days long irradiation, a cross-section limit of 0.58 pb was reached. Again, no decay chain that could be interpreted to originate from a $Z = 120$ isotope was observed [82, 83]. A third experiment was performed at TASCA, in the reaction $^{50}\text{Ti} + ^{249}\text{Cf}$. This is expected to be the most suitable one for $Z = 120$ synthesis from the reaction point of view [84]. In ≈ 39 days of irradiation, a cross-section limit of 0.2 pb was reached [85]. No genetically correlated α -decay chain that could be interpreted to originate from a $Z = 120$ isotope was observed. The fourth element 120 search experiment was conducted during the search for element 119 (see below).

2.2.2.2 Search for element 119

So far, the last attempt at GSI to synthesize an element beyond Og was a search for element 119 in the reaction $^{50}\text{Ti} + ^{249}\text{Bk}$ at TASCA [86]. The ^{249}Bk has a half-life of only 327.2 days. 12 mg of this isotope, produced at Oak Ridge National Laboratory, Oak Ridge, USA [5], became available in 2012. Targets were prepared at JGU (see Section 4.2) shortly after receiving the isotope. Irradiation started within about one month after target production. In a long run of about four months, no signature of element 119 was observed. This resulted in a cross-section limit of 65 fb [86]. The successful synthesis of element 119 in a future experiment apparently requires a considerably higher sensitivity.

In the course of the four-months experiment, ^{249}Bk continuously β^- decayed into ^{249}Cf . At the end, the ^{249}Cf content was about 35%. This provided a unique opportunity to simultaneously search for element 120. The beam energy was slightly lower (about 6 MeV) than the one used in the previous search experiment for element 120 in the $^{50}\text{Ti} + ^{249}\text{Cf}$ reaction. No α -decay chains that could be attributed to element 120 were observed, resulting in a ‘one event’ cross section limit of 0.2 pb [86].

3 Chemical studies to classify new elements in the periodic table

3.1 From actinides to the transactinide element 106, seaborgium, Sg

In 1985, the nuclear chemistry program began to focus on studies of the influence of RE on chemical properties of the heaviest elements and the architecture of the PTE [14–16,

87–89]. Prior experiments, performed in Berkeley and Dubna, had shown that $_{103}\text{Lr}$ behaved as expected for the last member of the actinide series and $_{104}\text{Rf}$ as a group-4 element. Now, the group-5 element $_{105}\text{Db}$ came into the focus and was studied. ARCA II was built [16, 90] to study 34-s ^{262}Db , and also 27-s ^{263}Db that was discovered in these experiments [89, 91, 92]. Db showed surprising chemical properties; simple extrapolations of chemical properties in the PTE did not yield trustworthy predictions anymore, but the properties were correctly predicted theoretically on the basis of fully relativistic calculations of group-5 complexes and explained by large SO effects on the 6d AOs causing a trend reversal in the group [88]. All experimental and theoretical results show that Db has chemical properties typical for a group 5 element.

The $_{106}\text{Sg}$ is placed in group 6 of the PTE, beneath Mo and W. Theoretical calculations [88] show that Sg has a $6d^47s^2$ ground state electronic configuration and the oxidation state 6+ in aqueous phases and in compounds accessible in gas phase studies [93]. The stability and behavior of many chemical compounds have been predicted [88, 94, 95]. Sg is expected to behave similarly to its lighter homologs.

After first work at FLNR [14], the chemical behavior of Sg was investigated by international collaborations at GSI using ARCA II [90] for studies in the aqueous phase and the On-Line Gas chemistry Apparatus (OLGA) III [15, 96] in the gas-phase. Theoretical results predicting stable dioxydichloride

compounds for group-6 elements and their volatility sequence of $\text{MoO}_2\text{Cl}_2 > \text{WO}_2\text{Cl}_2 > \text{SgO}_2\text{Cl}_2$ [94] motivated probing their formation and volatility. Advances in experimental techniques enabled studies with $\approx 10\text{-s}$ ^{265}Sg synthesized in the $^{22}\text{Ne} + ^{248}\text{Cm}$ reaction. Studies were carried out in liquid [97–99] and gaseous phases [97, 100, 101]. Nuclei, recoiling from the target, were thermalized in He, attached to aerosol particles and flushed to a quartz chromatography column within 3 s. Reactive gas was added to form volatile species. The yield of Sg passing the isothermal column at different temperatures was measured by registering Sg α decay chains [102]. The interaction strength of the species with the column material was determined, see Figure 8 [97, 100].

The obtained volatility sequence of $\text{MoO}_2\text{Cl}_2 > \text{WO}_2\text{Cl}_2 \approx \text{SgO}_2\text{Cl}_2$ and adsorption enthalpies ($-\Delta H_a$) of 90 ± 3 , 96 ± 1 , and 98^{+2}_-5 kJ/mol, respectively, were the first thermochemical information on Sg [100], and were in line with extrapolations in group 6 and with relativistic theory calculations [94]. Empirical correlations [103] yielded the sublimation enthalpy of a hypothetical Sg metal; this would be equal to or even higher than that of W, making Sg one of the least volatile elements. Later, the formation of Sg oxide hydroxide compounds was probed [101].

The chemistry of Sg in aqueous solutions [97–99] was studied on cation-exchange resin with ARCA II [14, 16, 90]. In the first experiments [97, 98], Sg eluted like Mo and W in 0.1 M $\text{HNO}_3/5 \times 10^{-4}$ M HF, unlike U. Thus, Sg is hexavalent, like a group-6 element. To shed more light on the formed compound, a second – and until today last – experiment was performed with pure HNO_3 [99]. Here, Sg was not observed in the W fraction, indicating that neutral or anionic oxyfluoride complexes were formed in the first study. Sg is the heaviest element studied in aqueous solution to date. The experiments were supported by fully-relativistic theoretical studies on the stability of oxidation states, complex formation and extraction from acidic solutions [88, 95].

The Sg chemistry experiments at GSI, including subsequent ones on Hs (see Section 3.2), and experiments at RIKEN yielded information on nuclear properties of ^{265}Sg and ^{266}Sg ; for a summary see Figure 9 and [67, 102, 104–106]. Isomeric states were found in ^{265}Sg and ^{261}Rf , and the conclusion was drawn that ^{266}Sg has not been observed before and was first synthesized as a daughter of ^{270}Hs [67].

Recently, the gas-phase formation of volatile group-6 element carbonyl complexes opened up novel types of SHE experiments. After exploratory studies [107] with fission-produced Mo thermalized in CO-containing gas at the TRIGA Mainz reactor [89, 108] and with W separated in TASCA at GSI, this technique was successfully applied in

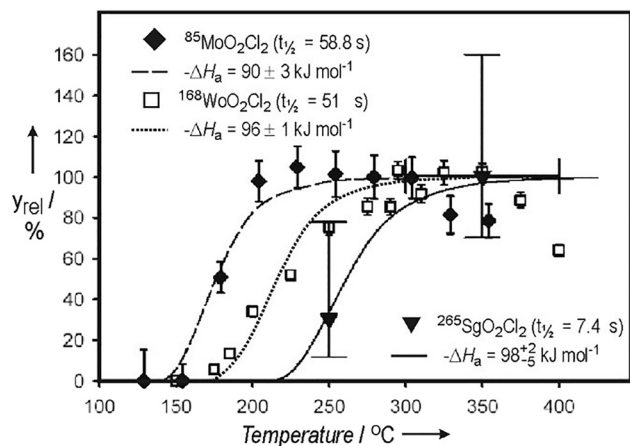


Figure 8: Relative yield, y_{rel} , of MO_2Cl_2 ($M = \text{Mo}, \text{W}$ and Sg) breaking through the column in OLGA III as a function of the isothermal temperature in the column. Adapted from [100]. (Reprinted figure with permission from WILEY-VCH from A. Türler et al., *Angew. Chem. Int. Ed.* 38, 2212–2213 (1999), [https://doi.org/10.1002/\(SICI\)1521-3773\(19990802\)38:15<2212::AID-ANIE2212>3.0.CO;2-6](https://doi.org/10.1002/(SICI)1521-3773(19990802)38:15<2212::AID-ANIE2212>3.0.CO;2-6). © WILEY-VCH Verlag GmbH, D-69,451 Weinheim, 1999).

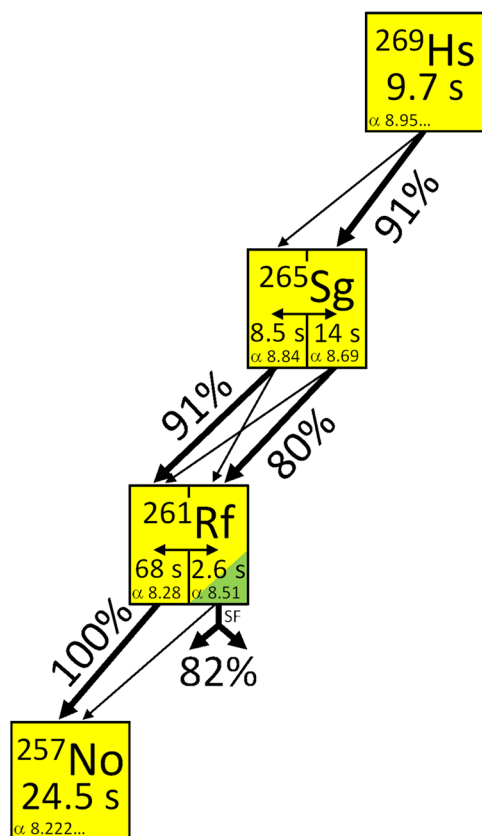


Figure 9: Decay pattern for the chain $^{269}\text{Hs} \rightarrow ^{265}\text{Sg}^{a,b} \rightarrow ^{261}\text{Rf}^{a,b} \rightarrow ^{257}\text{No}$. Yellow: α decay; green: spontaneous fission. The α -particle energies are given in MeV. The relative intensities of the decay branches are indicated by arrow thickness, and the intensity of the most intense branch is given. Data are from [104–106].

joint studies on $\text{Sg}(\text{CO})_6$ at RIKEN [89, 109]. Again, Sg behaved like a typical member of group 6. Theory works at GSI, predicting the behavior of carbonyl complexes of group 6–9 elements [11, 110], were confirmed.

3.2 Element 108, hassium, Hs

In 2001, the time was ripe for ^{108}Hs [111]. Applying novel techniques for irradiation, separation, and detection, all Hs chemistry experiments were conducted at GSI in international collaborations. They yielded chemical information on Hs, and also exciting nuclear results [112], see Figure 9, including evidence for the new isotope ^{270}Hs [67] – the first nuclide located on the $N = 162$ neutron-shell – and a confirmation of the Cn discovery by reproducing ^{277}Cn α -decay chains [74] from ^{269}Hs onwards.

The Hs homologs, Ru and Os, show a unique property: they exhibit oxidation state 8+, forming highly volatile tetroxides, attractive for gas-chemical studies of HsO_4

using ^{269}Hs produced via ^{26}Mg on ^{248}Cm . These differed from previous gas-phase studies: (i) The rotating target wheel ARTESIA [14] was used to allow highest beam intensities; (ii) The chemical reaction of Hs with O_2 in very dry He-gas was performed *in situ* behind the target [113], avoiding aerosol-jet transport; (iii) Instead of high-temperature chromatography, the cryo online detector (COLD), based on the technique developed at LBNL [114] was used. It consists of a thermochromatography channel formed by 36 pairs of silicon photodiodes kept at temperatures from -20°C at the inlet to -170°C at the exit [111]. Decay chains from ^{269}Hs were observed in a narrow peak [111, 112]; see Figure 10.

The observation of seven molecules of HsO_4 and their adsorption maximum at -44°C , in comparison with -82°C for OsO_4 , shows that Hs forms a relatively stable, volatile tetroxide [111]. HsO_4 adsorbed at higher temperature than OsO_4 , i.e., has a low volatility or high, negative adsorption enthalpy. This is in excellent agreement with the $-\Delta H_a$ value of 45.4 ± 1 kJ/mol obtained from improved fully relativistic 4-component density functional theory (4c-DFT) model calculations [115]. Relativistic calculations show that the trend in volatility and other properties established by RuO_4 and OsO_4 is reversed when going to HsO_4 . From Monte-Carlo simulations (solid lines in Figure 10) to the experimental data, the following values

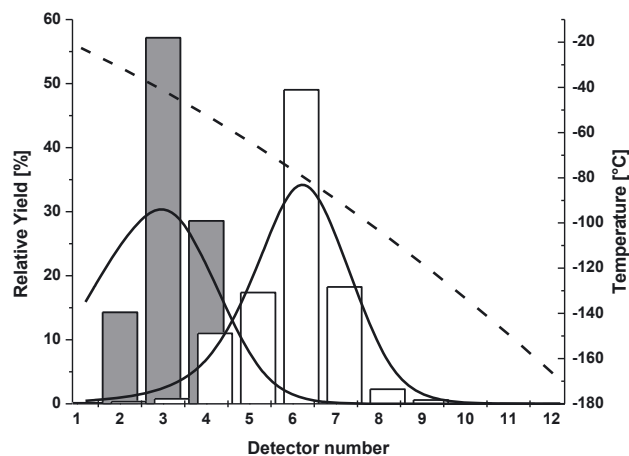


Figure 10: Experimentally observed thermochromatogram of HsO_4 (full histogram) and of OsO_4 (open histogram) as relative yields versus chromatography/detector number. One detector is 3 cm long. The dashed line shows the temperature profile. Solid lines represent results of Monte Carlo-simulations of the $^{269}\text{HsO}_4$ and $^{172}\text{OsO}_4$ migration along the temperature gradient assuming standard adsorption enthalpies of -46.0 kJ/mol and -39.0 kJ/mol, respectively. Taken from [111]. (Reprinted figure from Ch.E. Düllmann et al., Nature 418, 859–862 (2002), <https://doi.org/10.1038/nature00980>, with permission from Springer Nature).

(on silicon nitride) were deduced: $-\Delta H_a(\text{HsO}_4) = (46 \pm 2)$ kJ/mol and $-\Delta H_a(\text{OsO}_4) = (39 \pm 1)$ kJ/mol.

A second Hs chemistry experiment was performed using CALLISTO [89, 116]. Again, tetroxides were formed in a recoil chamber. This time H_2O vapor was added to the gas, which transported volatile products to detectors facing NaOH thin films. More than 50% of Os adsorbed opposite the first detector; one decay chain of Hs was detected in the first, one in the second, and three in the third detector [116]. Presumably, Hs deposits by forming a hassate(VIII) according to $2 \text{NaOH} + \text{HsO}_4 \rightarrow \text{Na}_2[\text{HsO}_4(\text{OH})_2]$. The low statistics constrains conclusions about the reactivity of HsO_4 as compared to OsO_4 . However, Os peaking earlier than Hs may indicate that HsO_4 is less reactive (more covalent) than OsO_4 [89], which would agree with theory [11]. For the first time, an acid-base chemical reaction was performed with HsO_4 [116]. All known Hs properties agree with its place in group 8.

Further thermochromatography experiments addressing nuclear aspects were performed using the Cryo-Online Multidetector for Physics and Chemistry of Transactinides (COMPACT) array [67, 112]. Obtained highlights include insights into the α decay of ^{269}Hs into two $^{265}\text{Sg}^{\text{a,b}}$ isomers, followed by α decays into two long-lived $^{261}\text{Rf}^{\text{a,b}}$ states (Figure 9) as well as the discoveries of $^{270,271}\text{Hs}$ and ^{266}Sg [67, 106, 112]. The Hs isotopes were produced with cross sections of 2–7 pb [106]. This showed for the first time that isotopes produced in the 1–10 pb range can be explored in chemical studies, which opened up a window to SHE around Fl. The properties of the ^{270}Hs decay chains were confirmed at the DGFERS and the half-life of ^{270}Hs was measured to 7.6 s [117]. The rather long half-lives, especially of the Sg and Hs isotopes, confirm the region of enhanced stability at around $Z = 108$ and $N = 162$ (see Section 2.2.1).

3.3 Element 113, nihonium, Nh and element 114, flerovium, Fl

In the past 15 years, $_{112}\text{Cn}$ and the main group elements beyond have come into the center of attention [11, 118, 119]. There are long-standing predictions, e.g. [120], that these elements should be volatile in the elemental state. This makes them amenable to gas phase chemical studies using setups similar as that used for the characterization of the highly volatile HsO_4 [111]. Particularly interesting are $_{112}\text{Cn}$ and $_{114}\text{Fl}$ in this respect. The reason for a high inertness of these elements is their closed and quasi-closed shell ground state electronic configurations, $6d^{10}7s^2$ and $7s^27p_{1/2}^2$, respectively, and a large relativistic stabilization

and contraction of the $7s$ and $7p_{1/2}$ AOs, making these orbitals less accessible for chemical bonding [121]. A relatively low reactivity of these elements towards Au and quartz, much lower than those of their 6th row homologs, was then predicted by fully relativistic periodic DFT calculations of their $-\Delta H_a$ on these surfaces [122–124] (see Figure 11). As a result, Fl should interact stronger with a gold surface than Cn, because of its active $7p$ AOs, while Cn is a closed-shell atom and should be relatively volatile (but not like Rn). In contrast, $_{113}\text{Nh}$ and $_{115}\text{Mc}$ should be chemically more reactive, due to one and three valence p-electrons, respectively, in the ground states. This is also confirmed by relativistic calculations of their $-\Delta H_a$ on Au and quartz [125] (Figure 11).

Relying on the expected high volatility and weak chemical reactivity, thermochromatography studies with COLD and COMPACT were performed for Cn and Fl, mainly on Au surfaces [119, 126, 128–130]. A noble-gas like behavior was derived from the pioneering chemistry experiment with Fl at the FLNR, based on the observation of three Fl atoms [128]. The unambiguous identification of single Fl atoms suffered from substantial background, which can be efficiently suppressed by using a recoil separator as a preseparator [131]. Preseparation is applied

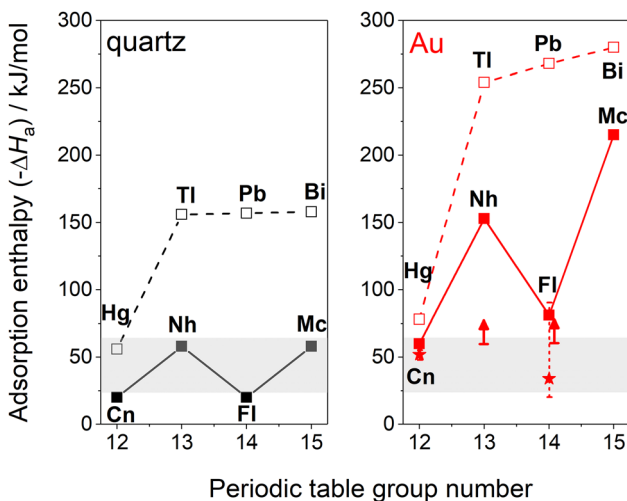


Figure 11: Theoretical and experimental values of adsorption enthalpy $-\Delta H_a$ on quartz (left panel, black symbols and lines) and Au (right panel, red symbols and lines) surfaces for the heaviest elements of the groups 12–15. Theoretical values (from [122, 123, 125]) are given by solid squares connected by solid lines for superheavy elements and by open squares connected by dashed lines for their homologs. Red star symbols and red arrows represent experimental adsorption enthalpy values on Au surfaces or their limits, respectively (from Refs. [126–130]). The grey marked areas represent the range, within which experimental values of $-\Delta H_a$ can be measured to date in an SHE chemistry experiment.

at GSI in chemistry experiments with elements beyond Hs [129, 130, 132] using the TASCA separator. First, two Fl atoms were registered on Au kept at room temperature, suggesting a metallic Fl-Au interaction [129]. In follow-up experiments, six further Fl atoms were observed [130], whereas several attempts at the FLNR did not result in the observation of Fl [119]. The Fl events measured in experiments at TASCA were distributed over two deposition zones: five of them were found on Au at room temperature, and three deposited at a low temperature on ice. An unambiguous explanation for the measured distribution will profit from additional data and extended theoretical work.

The $^{244}\text{Pu}(^{48}\text{Ca},3\text{-4n})^{288,289}\text{Fl}$ and $^{243}\text{Am}(^{48}\text{Ca},3\text{n})^{288}\text{Mc}$ reactions have similar cross sections, ≈ 10 pb [59]. The second member of the ^{288}Mc decay chain is ^{284}Nh ($T_{1/2} \approx 1$ s), which is accessible for chemical studies after an α decay of the short-lived mother nuclide ^{288}Mc ($T_{1/2} \approx 170$ ms). However, adsorption studies with Nh are likely more challenging than with Fl due to the higher reactivity of Nh atoms [125], which more easily leads to their loss on any surface they encounter before reaching the chromatography column. Pioneering Nh adsorption studies were performed at the FLNR [127]. A limit of $-\Delta H_a$ on Au was derived from the observation of five events, however, at high background conditions. Two attempts to measure the Nh adsorption behind a recoil separator were performed at the FLNR [133] and at TASCA [132], but no Nh events were observed. These results demonstrated additional challenges in studies of more reactive elements and called for the development of an advanced setup. The new miniCOMPACT detector array at TASCA, which does not require any transport line between the recoil transfer chamber and the detection setup [132], facilitates future gas-chromatography experiments on Nh and, possibly, even on Mc.

4 Targets for SHE synthesis

The SHE production is based on an intense heavy-ion beam impinging on a thin target, which has to withstand the beam-induced heating and structural modifications. The target material has to form a uniform layer with a well-defined layer thickness and sufficient mechanical stability to avoid loss of material during the – sometimes many months long – irradiation. Therefore, alongside the advancement of beam quality and intensity, the permanent improvement of the targets plays a key role to advance the field [134]. The target quality and the matching with experimental requirements are essential for heavy-element production.

For the heavy-element program at GSI, two set-ups are available: the SHIP separator and its ancillary setups, which focuses on physics experiments with stable targets, and the TASCA separator, where primarily actinide targets are used.

4.1 Targets of stable isotopes from the GSI target laboratory

For the majority of experiments on synthesis and investigation of nuclear properties of SHE using stable targets, the most frequently used ones include enriched Pb isotopes, mostly ^{208}Pb , as well as ^{209}Bi . Since Pb and Bi have low melting temperatures of 327 °C and 271 °C, respectively, increasing beam intensities that lead to larger energy deposition are challenging. During the history in heavy-element synthesis, major developments for the targets were necessary to ensure their durability under increasing beam intensity. The size of the active target area was increased to distribute the beam intensity over a target segment as wide as possible. The production process had to be adapted to keep the homogeneity of the target layer. Additionally, the rotation frequency of the wheel was optimized to fit to the pulsed beam structure of the UNILAC so that exactly the area of one target area is covered with one pulse, which has a typical duration of 5 ms. In addition, the shape of the beam-spot was refined to distribute the intensity more equally perpendicular to the rotation axis. Figure 12 shows a comparison of the new targets with the older version, each from the back and from the front side, respectively, before irradiation [135]. A major development to enhance the durability of the targets was substituting the metals by chemical compounds with higher melting points. For lead and bismuth, the most suitable compounds were found to be PbS and Bi_2O_3 with melting points of 1114 °C and 817 °C, respectively. For the PbS layers it turned out that a heating of the backing during the evaporation process was necessary to get a homogeneous compound layer [136].

Also, ^{238}U is a frequently used target material; here several alternatives are available via physical vapor deposition (PVD) methods. UF_4 can be evaporated from a tantalum crucible. Metallic U and UO_2 can be deposited with DC magnetron sputtering [137, 138]. While metallic U and UF_4 have melting points of 1132 °C and 1036 °C, respectively, the melting points of UO_2 (2865 °C) and UC (2375 °C) are significantly higher. In addition, metallic U oxidizes easily in (humid) air. Moreover, as most of the commercially available metallic U has already some oxygen impurity on delivery, further oxidation cannot not be hindered, even when the produced targets are kept in an inert atmosphere. Therefore, only a target of a high-melting

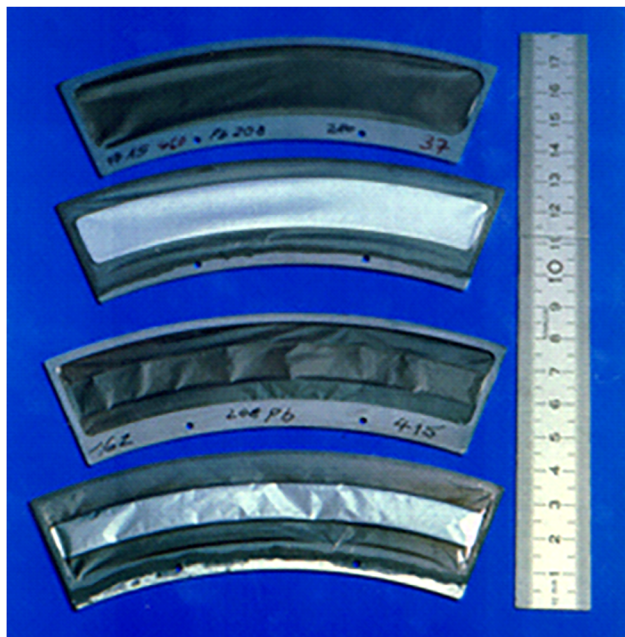


Figure 12: ^{208}Pb -targets on carbon backings for SHIP showing the backing side (1 and 3 from above) and the target side (2 and 4 from above), respectively, with an enlarged target area and improved backing quality (upper two) compared to the previous target version (lower two) [135]. (Reprinted from B. Lommel et al., Nucl. Instrum. Meth. A 480, 16–21 (2002), “Improvement of the target durability for heavy-element production”, [https://doi.org/10.1016/S0168-9002\(01\)02041-1](https://doi.org/10.1016/S0168-9002(01)02041-1), © 2002, with permission from Elsevier.).

uranium compound, which is stable in air, guarantees for long lasting stability. Currently, however, obtaining depleted material in high purity in the desired compound form as a sputtering target is a major problem.

For all the target materials mentioned above, amorphous C with a thickness between 30 and 40 $\mu\text{g}/\text{cm}^2$ is the backing of choice [139]. Additionally, the target layer is covered with a thin C layer to minimize target losses from sputtering. The lanthanides are also interesting target materials for spectroscopic investigations of lighter elements, and also for chemical studies, because they lead to the lighter homologs of the SHE that are produced with actinide targets. Here, nearly all lanthanides are produced by thermal evaporation as lanthanide fluoride on C backing. For the production of actinide targets, different combinations of backings and compounds were tested [140].

4.2 Actinide targets from the Mainz nuclear chemistry lab

In contrast to Pb and Bi and basically any natural isotope, transuranium isotopes are produced artificially. Many,

especially of transplutonium elements, are therefore only available in minute quantities [5], which limits the applicable methods for target production. The “molecular plating” (MP) method [141] fulfills the requirements of high efficiency, target stability, the option to reprocess irradiated targets, and is applicable to actinides. The MP is based on an electrochemical deposition of dissolved material from an alcoholic solution by applying a constant current between an anode and the supporting substrate, which is biased as a cathode. By adapting, e.g., the applied current and time, the method is capable to produce homogeneous layers of various actinide elements from U up to Cf with thicknesses up to about 1 mg/cm^2 and yields of 90% or more in a single deposition step [142–144]. In the past, thin foils of Be, C, Ta or Pt have mostly been used as substrate for the actinide layer. Currently $\approx 2.2\ \mu\text{m}$ Ti foils are favored; these offer a good compromise between a minimal thickness to minimize the energy loss of the ion beam, and sufficient mechanical and thermal resistance to survive the target production process as well as the harsh conditions during irradiation. Figure 13 shows an exemplary target wheel with four ^{249}Bk segments, which were used for experiments on Ts [78] and the search for element 119 [86] at TASCA.

Key parameters of the production process and relevant layer parameters are determined by using various analytical



Figure 13: Assembled TASCA target wheel with four target segments, containing a total amount of about 12 mg ^{249}Bk , deposited by molecular plating on 2 μm Ti backings [144]. The total ^{249}Bk β^- -activity was $6 \cdot 10^{11}$ Bq at the beginning of irradiation [86]. (Reprinted by permission from Springer nature Customer Service Centre GmbH: Nature Springer J. Radioanal. Nucl. Chem. 299, 1081–1804 (2014), “Preparation of actinide targets for the synthesis of the heaviest elements”, <https://doi.org/10.1007/s10967-013-2616-6>, J. Runke et al., © 2014).

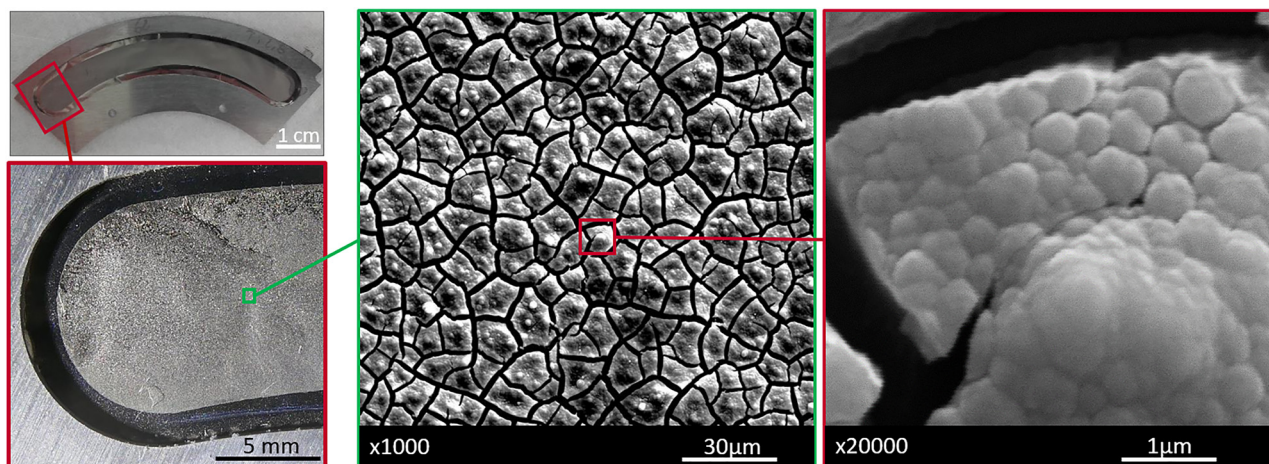


Figure 14: Photographies (top and bottom left) and SEM pictures (center and right) of a $500 \mu\text{g}/\text{cm}^2$ La target on a TASCA target frame.

techniques. These include deposition yield determination via α and γ -spectroscopy, either of the finished target (direct determination) or of the supernatant solution (indirect determination). If stable or very long-lived nuclides are used, γ -spectrometry of neutron-activated samples can provide similar information. Radiographic imaging provides qualitative information of the homogeneity of radioactive layers. Further microscopic techniques include atomic force microscopy (AFM), which reveals the morphology and roughness of a target on a micrometer scale, and scanning electron microscopy (SEM), which allows taking detailed pictures of representative structures on the target (see Figure 14). This helps benchmarking the influence of specific plating parameters (e.g., used solvent, current density, deposition time) on the produced layers. In combination with an energy-dispersive X-ray (EDX) detector, elemental analysis of the layer can be performed.

Although MP has been used for many decades in the SHE community, comprehensive analytics of the properties of layers produced by this method and the chemical and physical changes induced by extended exposures to intense heavy-ion beams are still incomplete and have become a field of interest in the last decade [145, 146]. The aim is to get a better understanding of the MP process and the properties of the produced layers, which shall serve as a basis to advance target production methods. One avenue goes into the direction of more modern electrochemical approaches, known in literature for lanthanide chemistry [147–149]. Such methods have the potential (i) to give access to more beam-resistant targets, (ii) to provide layers of thicknesses in excess of $1 \text{ mg}/\text{cm}^2$, (iii) to avoid unwanted structural inhomogeneities caused, e.g., by mud-cracking effects, and (iv) to provide layers with a better defined chemical structure. Further work addresses the backing.

5 Outlook and perspectives

SHE research at the GSI will continue to address open key questions in the field like pinning down the exact location and extension of the island of stability and exploration of the limits of nuclear stability and of the PTE, as well as studying how well the SHE fit into the structure of the PTE. The connection of GSI to JGU has been strengthened with the foundation of the joint daughter Helmholtz Institute Mainz (HIM) on June 9, 2010. HIM is an outpost of GSI located on the JGU campus. Accelerator development as well as SHE research are pillars of the HIM research mission. In a continuation of current research activities, which are much broader than the focus described in this article, a comprehensive program studying production, nuclear, chemical, and atomic properties of superheavy nuclides will form the core of the activities in Darmstadt in the next decades.

Fusion-evaporation reactions with stables beams remain key to access the region of highest Z and A as the intensities of radioactive beams are presently too low to produce SHN. Producing elements beyond Og in fusion-evaporation reactions requires projectiles beyond ^{48}Ca , as no target material with $Z > 98$ is available in sufficient quantity. Based on theoretical predictions and on current experimental upper limits, cross-sections of 0.01 pb or below are expected. Thus, a substantial increase in beam intensity will be crucial to carry out promising search experiments within acceptable experiment durations. More neutron-rich isotopes may become accessible in multi-nucleon transfer reactions [89].

An order of magnitude higher beam intensity compared to the UNILAC is expected from a future HELmholtz LInear ACcelerator (HELIAC) [150], for which R&D activities are

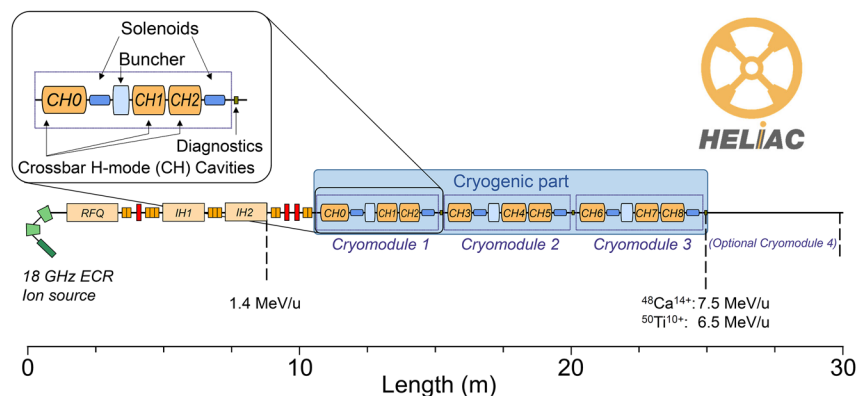


Figure 15: Schematic layout of the HELIAC linear accelerator in the full SHE configuration. ECR, Electron-cyclotron resonance; RFQ, Radio-frequency quadrupole IH, Interdigital H-mode cavity. Bunchers for longitudinal beam focusing are indicated by red boxes and doublets and triplets of quadrupole magnets for transversal beam focusing by orange square boxes. Addition of a 4th cryomodule to reach higher energies is most relevant for applications outside of SHE research. Typical projectiles are indicated along with the maximum reachable energies for the given charge states.

ongoing and first components are being commissioned. A schematic of the HELIAC in an envisaged configuration with continuous wave beams for SHE research is depicted in Figure 15. Activities towards a first, intermediate step, where the operational parameters will be similar to those of UNILAC, are currently ongoing.

Higher beam currents necessitate further developments of the target technology. Detailed studies of the properties and performance of (actinide) targets from different production methods and the development of new target production technologies are under way at JGU.

The recoil separators and detection systems are constantly being upgraded for increased sensitivity and efficiency. State-of-the-art digital signal processing for dead-time free data acquisition [57, 151] will be used and will be optimized for detecting low-energy conversion electrons [152] and electron-capture decays that will play an increasingly important role in SHN that are more neutron-rich than the currently known ones and will be located closer to the beta-stability line.

New spectroscopy setups are under construction. The new LUNDIUM detector is a next-generation spectroscopy setup based on separating ERs in a recoil separator and implanting them in a highly granular Si detector surrounded by pixelized box detectors (cf. Section 2.2.1), which are monitored by highly efficient multi-segment photon detectors [153]. In contrast, in the so-called diffusion-controlled adsorption technique, ERs are extracted from the separator, thermalized in a gas-filled volume and flushed into a narrow channel built from Si detector arrays similar to those used for chemical studies of HsO₄ and the elements Cn and beyond (cf. Sections 3.2 and 3.3 and Figure 10). Non-volatile species adsorb quantitatively upon

first contact; particles and photons emitted in their decay can efficiently be registered in the Si detectors and in closely positioned high-efficiency Ge detectors, as was recently demonstrated with a proof-of-concept prototype. This technique will allow to explore simultaneously chemical as well as physical properties of SHN, including processes, which were previously almost inaccessible, e.g., fission fragment mass distribution from spontaneously fissioning SHN. The new setups will provide more options for the direct identification of Z of new elements by the registration of α -X-ray correlations. Alpha-photon spectroscopy of the SHN will provide important nuclear structure data. Recently, decay chains starting at Fl were studied in this way [154] using the TASI Spec+ detector, an intermediate upgrade of the “TASCA in Small Image mode Spectroscopy” (TASI Spec) setup [155] towards LUNDIUM. In these studies, the observed α -decay energies attributed to even–even decay chains ${}_{116}\text{Lv}-{}_{114}\text{Fl}-{}_{112}\text{Cn}$ do not show a kink; this, though, is a typical signature for a shell closure. The absence of a kink indicates that no pronounced shell effect from crossing $Z = 114$ is observed at $N = 174$ [89,154].

Future chemical studies at TASCA will profit from next-generation equipment [132] and higher beam intensity. More short-lived isotopes will come into reach by coupling fast chemistry setups with a novel Universal high-density gas stopping Cell (UniCell) [156], promising access to elements beyond Fl as well as the still neglected elements with $Z = 109-111$.

Further observables of SHE are probed in precision measurements by mass spectrometry with SHIPTRAP and by laser spectroscopy [157]; these techniques have reached Db and Lr, respectively, and will be advanced to heavier elements. Besides providing accurate masses, long-lived

isomeric states with excitation energies of only tens of keV can be identified with SHIPTRAP. Laser spectroscopy will provide information on nuclear spins, electromagnetic moments, changes in mean-square charge radii, and in some cases reveal the configuration of isomers. The comprehensive exploration of superheavy elements and their isotopes will remain a strong pillar of the scientific program at Darmstadt.

Acknowledgments: The results and perspectives summarized in this article would not have been possible without the hard work of all staff within the GSI groups working in physics and chemistry of the heaviest elements and in associated groups including the ion source and accelerator departments, the experiment electronics department, the target laboratory, the nuclear chemistry groups at JGU Mainz, and more recently also at HIM. International collaboration partners from all over the world made essential contributions to the experiments at GSI. We are grateful for the continuous strong support from the GSI directorate and for funding that superheavy element research obtained over the decades from a variety of funding agencies.

Author contributions: All the authors have accepted responsibility for the entire content of this submitted manuscript and approved submission.

Research funding: None declared.

Conflict of interest statement: The authors declare no conflicts of interest regarding this article.

References

1. McMillan E., Abelson P. H. Radioactive element 93. *Phys. Rev.* 1940, *57*, 1185–1186.
2. Sobczewski A., Gareev F. A., Kalinkin B. N. Closed shells for $Z > 82$ and $N > 126$ in a diffuse potential well. *Phys. Lett.* 1966, *22*, 500–502.
3. Myers W. D., Swiatecki W. J. Nuclear masses and deformations. *Nucl. Phys.* 1966, *81*, 1–60.
4. Nilsson S. G., Nix J. R., Sobczewski A., Szymanski Z., Wycech S., Gustafson C., Möller P. On the spontaneous fission of nuclei with Z near 114 and N near 184. *Nucl. Phys.* 1968, *A115*, 545–562.
5. Roberto J. B., Alexander C. W., Boll R. A., Burns J. D., Ezold J. G., Felker L. K., Hogle S. L., Rykaczewski K. P. Actinide targets for the synthesis of super-heavy elements. *Nucl. Phys. A* 2015, *944*, 99–116.
6. Armbruster P., Münzenberg G. An experimental paradigm opening the world of superheavy elements. *Eur. Phys. J. H* 2012, *37*, 237–309.
7. Münzenberg G., Faust W., Hofmann S., Armbruster P., Güttner K., Ewald H. The velocity filter SHIP, a separator of unslowed heavy ion fusion products. *Nucl. Instrum. Methods* 1979, *161*, 65–82.
8. Chatt J. Recommendations for the naming of elements of atomic numbers greater than 100. *Pure Appl. Chem.* 1979, *51*, 381–384.
9. Pyykkö P., Desclaux J.-P. Relativity and the periodic system of elements. *Acc. Chem. Res.* 1979, *12*, 276–281.
10. Fricke B., Waber J. Theoretical predictions of the chemistry of superheavy elements. Continuation of the periodic table up to $Z = 184$. *Actinides Rev* 1971, *1*, 433–485.
11. Pershina V. Relativity in the electronic structure of the heaviest elements and its influence on periodicities in properties. *Radiochim. Acta* 2019, *107*, 833–863.
12. Heinz S., Devaraja H. M., Beliuskina O., Comas V., Hofmann S., Hornung C., Münzenberg G., Ackermann D., Gupta M., Henderson R. A., Heßberger F. P., Kindler B., Lommel B., Mann R., Maurer J., Moody K. J., Nishio K., Popeko A. G., Shaughnessy D. A., Stoyer M. A., Yeremin A. V. Synthesis of new transuranium isotopes in multinucleon transfer reactions using a velocity filter. *Eur. Phys. J. A* 2016, *52*, 278.
13. Di Nitto A., Khuyagbaatar J., Ackermann D., Andersson L.-L., Badura E., Block M., Brand H., Conrad I., Cox D. M., Düllmann Ch. E., Dvorak J., Eberhardt K., Ellison P. A., Esker N. E., Even J., Fahlander C., Forsberg U., Gates J. M., Golubev P., Gothe O., Gregorich K. E., Hartmann W., Herzberg R.-D., Heßberger F. P., Hoffmann J., Hollinger R., Hübner A., Jäger E., Kindler B., Klein S., Kojouharov I., Kratz J. V., Krier J., Kurz N., Lahiri S., Lommel B., Maiti M., Mändl R., Merchán E., Minami S., Mistry A. K., Mokry C., Nitsche H., Omtvedt J. P., Pang G. K., Renisch D., Rudolph D., Runke J., Sarmiento L. G., Schädel M., Schaffner H., Schausten B., Semchenkov A., Steiner J., Thörle-Pospiech P., Trautmann N., Türlér A., Uusitalo J., Ward D., Wegrzecki M., Wieczorek P., Wiehl N., Yakushev A., Yakusheva V. Study of non-fusion products in the $^{50}\text{Ti} + ^{249}\text{Cf}$ reaction. *Phys. Lett. B* 2018, *784*, 199–205.
14. Schädel M. Chemistry of the superheavy elements. *Angew. Chem. Int. Ed.* 2006, *45*, 368–401.
15. Türlér A., Pershina V. Advances in the production and chemistry of the heaviest elements. *Chem. Rev.* 2013, *113*, 1237–1312.
16. Schädel M., Nagame Y. From SRAFAP to ARCA and AIDA – developments and implementation of automated aqueous-phase rapid chemistry apparatuses for heavy actinides and transactinides. *Radiochim. Acta* 2019, *107*, 561–585.
17. Heßberger F. P. Nuclear structure investigations in the region of superheavy nuclei. *Phys. At. Nuclei* 2007, *70*, 1445–1451.
18. Asai M., Heßberger F. P., Lopez-Martens A. Nuclear structure of elements with $100 \leq Z \leq 109$ from alpha spectroscopy. *Nucl. Phys. A* 2015, *944*, 308–332.
19. Heßberger F. P. Nuclear structure of the transactinides – investigated by decay spectroscopy. *EPJ Web Conf.* 2016, *131*, 02005.
20. Block M., Ackermann D., Blaum K., Droese C., Dworschak M., Eliseev S., Fleckenstein T., Haettner E., Herfurth F., Heßberger F. P., Hofmann S., Ketelaer J., Ketter J., Kluge H.-J., Marx G., Mazzocco M., Novikov Y. N., Plaß W. R., Popeko A., Rahaman S., Rodríguez D., Scheidenberger C., Schweikhard L., Thirof P. G., Vorobyev G. K., Weber C. Direct mass measurements above uranium bridge the gap to the island of stability. *Nature* 2010, *463*, 785–788.
21. Kaleja O., Andelić B., Blaum K., Block M., Chhetri P., Droese C., Düllmann Ch. E., Eibach M., Eliseev S., Even J., Götz S., Giacoppo F., Kalantar-Nayestanaki N., Laatiaoui M., Ramirez E. M., Mistry A., Murböck T., Raeder S., Schweikhard L.,

- Thirolf P. G. The performance of the cryogenic buffer-gas stopping cell of SHIPTRAP. *Nucl. Instrum. Methods Phys. Res. B* 2020, 463, 280–285.
22. Block M. Precise ground state properties of the heaviest elements for studies of their atomic and nuclear structure. *Radiochim. Acta* 2019, 107, 603–613.
23. Ramirez E. M., Ackermann D., Blaum K., Block M., Droese C., Düllmann Ch. E., Dworschak M., Eibach M., Eliseev S., Haettner E., Herfurth F., Heßberger F. P., Hofmann S., Ketelaer J., Marx G., Mazzocco M., Nesterenko D., Novikov Y. N., Plaß W. R., Rodríguez D., Scheidenberger C., Schweikhard L., Thirolf P. G., Weber C. Direct mapping of nuclear shell effects in the heaviest elements. *Science* 2012, 337, 1207–1210.
24. Block M., Laatiaoui M., Raeder S. Recent progress in laser spectroscopy of the actinides. *Prog. Part. Nucl. Phys.* 2021, 116, 103834.
25. Lauth W., Backe H., Dahlinger M., Klafit I., Schwamb P., Schwickert G., Trautmann N., Othmer U. Resonance ionization spectroscopy in a buffer gas cell with radioactive decay detection, demonstrated using ^{208}Tl . *Phys. Rev. Lett.* 1992, 68, 1675–1678.
26. Raeder S., Ackermann D., Backe H., Beerwerth R., Berengut J. C., Block M., Borschevsky A., Cheal B., Chhetri P., Düllmann Ch. E., Dzuba V. A., Eliav E., Even J., Ferrer R., Flambaum V. V., Fritzsche S., Giacompo F., Götz S., Heßberger F. P., Huysse M., Kaldor U., Kaleja O., Khuyagbaatar J., Kunz P., Laatiaoui M., Lautenschläger F., Lauth W., Mistry A. K., Ramirez E. M., Nazarewicz W., Porsev S. G., Safronova M. S., Safronova U. I., Schuettrumpf B., Duppen P. V., Walther T., Wraith C., Yakushev A. Probing sizes and shapes of nobelium isotopes by laser spectroscopy. *Phys. Rev. Lett.* 2018, 120, 232503.
27. Chhetri P., Ackermann D., Backe H., Block M., Cheal B., Droese C., Düllmann Ch. E., Even J., Ferrer R., Giacompo F., Götz S., Heßberger F. P., Huysse M., Kaleja O., Khuyagbaatar J., Kunz P., Laatiaoui M., Lautenschläger F., Lauth W., Lecesne N., Lens L., Ramirez E. M., Mistry A. K., Raeder S., Duppen P. V., Walther T., Yakushev A., Zhang Z. Precision measurement of the first ionization potential of nobelium. *Phys. Rev. Lett.* 2018, 120, 263003.
28. Düllmann Ch. E., Herzberg R.-D., Nazarewicz W., Oganessian Y., Special issue on superheavy elements. *Nucl. Phys. A* 2015, 944.
29. Herrmann G. Historical reminiscences. In *The Chemistry of Superheavy Elements*; Schädel M., Shaughnessy D., Eds.; Springer: Heidelberg, 2014, pp. 485–511.
30. Gäggeler H., Trautmann N., Bröchle W., Herrmann G., Kratz J. V., Peuser P., Schädel M., Tittel G., Wirth G., Ahrens H., Folger H., Franz G., Sümmerer K., Zündel M. Search for superheavy elements in the $^{238}\text{U} + ^{238}\text{U}$ reaction. *Phys. Rev. Lett.* 1980, 45, 1824–1827.
31. Herrmann G. Synthesis of the heaviest chemical elements - results and perspectives. *Angew. Chem. Int. Ed.* 1988, 27, 1417–1436.
32. Kratz J. V. The search for superheavy elements. *Radiochim. Acta* 1983, 32, 25–41.
33. Schädel M., Bröchle W., Haefner B., Kratz J. V., Schorstein W., Trautmann N., Herrmann G. Chemical separations of actinide elements from heavy-ion irradiated uranium targets. *Radiochim. Acta* 1978, 25, 111–117.
34. Schädel M., Kratz J. V., Ahrends H., Bröchle W., Franz G., Gäggeler H., Warnecke I., Wirth G., Herrmann G., Trautmann N., Weis M. Isotope distributions in the reaction $^{238}\text{U} + ^{238}\text{U}$. *Phys. Rev. Lett.* 1978, 41, 469–472.
35. Kratz J. V., Schädel M., Gäggeler H. W. Reexamining the heavy-ion reactions $^{238}\text{U} + ^{238}\text{U}$ and $^{238}\text{U} + ^{248}\text{Cm}$ and actinide production close to the barrier. *Phys. Rev. C* 2013, 88, 054615.
36. Kratz J. V. Nuclear and Radiochemistry – Fundamentals and Applications, 4th ed., *Chapter 12 nuclear reactions.*; Wiley VCH: Weinheim, Germany, 2021; pp 361–488.
37. Riedel C., Nörenberg W. Theoretical estimates for the production of transuranium elements in heavy-ion collisions. *Z. Phys. A* 1979, 290, 385–391.
38. Schädel M., Bröchle W., Gäggeler H., Kratz J. V., Sümmerer K., Wirth G., Herrmann G., Stakemann R., Tittel G., Trautmann N., Nitschke J. M., Hulet E. K., Loughheed R. W., Hahn R. L., Ferguson R. L. Actinide production in collisions of ^{238}U with ^{248}Cm . *Phys. Rev. Lett.* 1982, 48, 852–855.
39. Zagrebaev V., Greiner W. Synthesis of superheavy nuclei: a search for new production reactions. *Phys. Rev. C* 2008, 78, 034610.
40. Zagrebaev V. I., Greiner W. Production of heavy and superheavy neutron-rich nuclei in transfer reactions. *Phys. Rev. C* 2011, 83, 044618.
41. Armbruster P., Agarwal Y. K., Bröchle W., Brügger M., Dufour J. P., Gäggeler H., Hessberger F. P., Hofmann S., Lemmert P., Münzenberg G., Poppensieker K., Reisdorf W., Schädel M., Schmidt K. H., Schneider J. H. R., Schneider W. F. W., Sümmerer K., Vermeulen D., Wirth G., Ghiorso A., Gregorich K. E., Lee D., Leino M., Moody K. J., Seaborg G. T., Welch R. B., Wilmarth P. Attempts to produce superheavy elements by fusion of ^{48}Ca with ^{248}Cm in the bombarding energy range of 4.5–5.2 MeV/u. *Phys. Rev. Lett.* 1985, 54, 406–409.
42. Gäggeler H., Bröchle W., Brügger M., Schädel M., Sümmerer K., Wirth G., Kratz J. V., Lerch M., Blaich T., Herrmann G., Hildebrand N., Trautmann N., Lee D., Moody K. J., Gregorich K. E., Welch R. B., Seaborg G. T., Hoffman D. C., Daniels W. R., Fowler M. M., von Gunten H. R. Production of cold target-like fragments in the reaction of $^{48}\text{Ca} + ^{248}\text{Cm}$. *Phys. Rev. C* 1986, 33, 1983–1987.
43. Schädel M., Bröchle W., Haefner B. Fast radiochemical separations with an automated rapid chemistry apparatus. *Nucl. Instrum. Methods Phys. Res., Sect. A* 1988, 264, 308–318.
44. Hoffman D. C., Fowler M. M., Daniels W. R., von Gunten H. R., Lee D., Moody K. J., Gregorich K., Welch R., Seaborg G. T., Bröchle W., Brügger M., Gäggeler H., Schädel M., Sümmerer K., Wirth G., Blaich T., Herrmann G., Hildebrand N., Kratz J. V., Lerch M., Trautmann N. Excitation functions for production of heavy actinides from interactions of ^{40}Ca and ^{48}Ca ions with ^{248}Cm . *Phys. Rev. C* 1985, 31, 1763.
45. Loughheed R. W., Landrum J. H., Hulet E. K., Wild J. F., Dougan R. J., Dougan A. D., Gäggeler H., Schädel M., Moody K. J., Gregorich K. E., Seaborg G. T. Search for superheavy elements using the $^{48}\text{Ca} + ^{254}\text{Es}^{\text{g}}$ reaction. *Phys. Rev. C* 1985, 32, 1760–1763.
46. Schädel M., Jäger E., Bröchle W., Sümmerer K., Hulet E. K., Wild J. F., Loughheed R. W., Dougan R. J., Moody K. J. Radiochemical search for neutron-rich isotopes of nielsbohrium in the $^{16}\text{O} + ^{254}\text{Es}$ reaction. *Radiochim. Acta* 1995, 68, 7–12.
47. Schädel M., Bröchle W., Brügger M., Gäggeler H., Moody K. J., Schardt D., Sümmerer K., Hulet E. K., Dougan A. D., Dougan R. J., Landrum J. H., Loughheed R. W., Wild J. F., O’Kelley G. D. Transfer cross sections from reactions with ^{254}Es as a target. *Phys. Rev. C* 1986, 33, 1547–1550.

48. Moody K. J., Bröchle W., Brügger M., Gäggeler H., Haefner B., Schädel M., Sümmerer K., Tetzlaff H., Herrmann G., Kaffrell N., Kratz J. V., Rogowski J., Trautmann N., Skälberg M., Skarnemark G., Alstad J., Fowler M. M. New nuclides: neptunium-243 and neptunium-244. *Z. Phys.* 1987, **328**, 417–422.
49. Hofmann S., Münzenberg G. The discovery of the heaviest elements. *Rev. Mod. Phys.* 2000, **72**, 733–767.
50. Hofmann S., Münzenberg G., Hessberger F. P., Schött H. J. Detector system for investigation of proton radioactivity and new elements at SHIP. *Nucl. Instrum. Meth. Phys. Res.* 1984, **223**, 312–318.
51. Münzenberg G., Armbruster P., Heßberger F. P., Hofmann S., Poppensieker K., Reisdorf W., Schneider J. H. R., Schneider W. F. W., Schmidt K. H., Sahm C. C., Vermeulen D. Observation of one correlated α -decay in the reaction ^{58}Fe on $^{209}\text{Bi} \rightarrow ^{267}\text{109}$. *Z. Phys. A* 1982, **309**, 89–90.
52. Strutinski V. M. Shell effects in nuclear masses and deformation energies. *Nucl. Phys.* 1967, **A95**, 420–442.
53. Čwiok S., Pashkevich V. V., Dudek J., Nazarewicz W. Fission barriers of transfermium elements. *Nucl. Phys.* 1983, **A410**, 254–270.
54. Patyk Z., Sobiczewski A. Ground-state properties of the heaviest nuclei analyzed in a multidimensional deformation space. *Nucl. Phys.* 1991, **A533**, 132–152.
55. Semchenkov A., Bröchle W., Jäger E., Schimpf E., Schädel M., Mühle C., Klos F., Türler A., Yakushev A., Belov A., Beyakova T., Kaparkova M., Kukhtin V., Lamzin E., Sytchevsky S. The TransActinide Separator and Chemistry Apparatus (TASCA) at GSI – optimization of ion-optical structures and magnet designs. *Nucl. Instrum. Methods Phys. Res. B* 2008, **266**, 4153–4161.
56. Münzenberg G., Armbruster P., Berthes G., Hessberger F. P., Hofmann S., Reisdorf W., Schmidt K. H., Schött H. J. The experimental work at the velocity filter SHIP – Results and plans. *Nucl. Instrum. Methods* 1987, **B26**, 294–300.
57. Khuyagbaatar J., Yakushev A., Düllmann Ch. E., Ackermann D., Andersson L.-L., Asai M., Block M., Boll R. A., Brand H., Cox D. M., Dasgupta M., Derkx X., Di Nitto A., Eberhardt K., Even J., Evers M., Fahlander C., Forsberg U., Gates J. M., Gharibyan N., Golubev P., Gregorich K. E., Hamilton J. H., Hartmann W., Herzberg R.-D., Heßberger F. P., Hinde D. J., Hoffmann J., Hollinger R., Hübner A., Jäger E., Kindler B., Kratz J. V., Krier J., Kurz N., Laatiaoui M., Lahiri S., Lommel R. L. B., Maiti M., Miernik K., Minami S., Mistry A., Mokry C., Nitsche H., Omtvedt J. P., Pang G. K., Papadakis P., Renisch D., Roberto J., Rudolph D., Runke J., Rykaczewski K. P., Sarmiento L. G., Schädel M., Schausten B., Semchenkov A., Shaughnessy D. A., Steinegger P., Steiner J., Tereshatov E. E., Thörle-Pospiech P., Tinschert K., Torres De Heidenreich T., Trautmann N., Türler A., Uusitalo J., Ward D. E., Wegrzecki M., Wiehl N., Van Cleve S. M., Yakusheva V. Fusion reaction $^{48}\text{Ca} + ^{249}\text{Bk}$ leading to formation of the element Ts ($Z = 117$). *Phys. Rev. C* 2019, **99**, 054306.
58. Morita K., Morimoto K., Kaji D., Haba H., Ozeki K., Kudou Y., Sumita T., Wakabayashi Y., Yoneda A., Tanaka K., Yamaki S., Sakai R., Akiyama T., Goto S., Hasebe H., Huang M., Huang T., Ideguchi E., Kasamatsu Y., Katori K., Kariya Y., Kikunaga H., Koura H., Kudo H., Mashiko A., Mayama K., Mitsuoka S., Moriya T., Murakami M., Murayama H., Namai S., Ozawa A., Sato N., Sueki K., Takeyama M., Tokanai F., Yoshida A. New result in the production and decay of an isotope, $^{278}\text{113}$, of the 113th element. *J. Phys. Soc. Jpn.* 2012, **81**, 103201.
59. Oganessian Y. T., Utyonkov V. K. Super-heavy element research. *Rep. Prog. Phys.* 2015, **78**, 036301.
60. Münzenberg G., Armbruster P., Hofmann S., Heßberger F. P., Folger H., Keller H., Ninov V., Poppensieker K., Quint A. B., Reisdorf W., Schmidt K. H., Schneider J. H. R., Schött H. J., Sümmerer K., Zychor I., Leino M. E., Ackermann D. G., Hanelt E., Morawek W., Vermuelen D., Fujita Y., Schwab T. Element 107. *Z. Phys. A* 1989, **333**, 163–175.
61. Münzenberg G., Reisdorf W., Hofmann S., Agarwal Y. K., Heßberger F. P., Poppensieker K., Schneider J. H. R., Schneider W. F. W., Schmidt K. H., Schött H.-J., Armbruster P., Sahm C. C., Vermeulen D. Evidence for element 109 from one correlated decay sequence following the fusion of ^{58}Fe with ^{209}Bi . *Z. Phys. A* 1984, **315**, 145–158.
62. Oganessian Y. T., Hussonnois M., Demin A. G., Kharitonov Y. P., Bruchertseifer H., Constantinescu O., Korotkin Y. S., Tretyakova S. P., Utyonkov V. K., Shirokovsky I. V., Estevez J. Experimental studies of the formation and radioactive decay of isotopes with $Z = 104$ – 109 . *Radiochim. Acta* 1984, **37**, 113–120.
63. Münzenberg G., Hofmann S., Heßberger F. P., Folger H., Ninov V., Poppensieker K., Quint A. B., Reisdorf W., Schött H.-J., Sümmerer K., Armbruster P., Leino M. E., Ackermann D., Gollerthan U., Hanelt E., Morawek W., Fujita Y., Schwab T., Türler A. New results on element 109. *Z. Phys. A* 1988, **330**, 435–436.
64. Hofmann S., Heßberger F. P., Ninov V., Armbruster P., Münzenberg G., Stodel C., Popeko A. G., Yerebin A. V., Saro S., Leino M. Excitation function for the production of $^{265}\text{108}$ and $^{266}\text{109}$. *Z. Phys. A* 1997, **358**, 377–378.
65. Münzenberg G., Armbruster P., Folger H., Heßberger F. P., Hofmann S., Keller J., Poppensieker K., Reisdorf W., Schmidt K.-H., Schött H.-J. The identification of element 108. *Z. Phys. A* 1984, **317**, 235–236.
66. Randrup J., Larsson S. E., Möller P., Nilsson S. G., Pomorski K., Sobiczewski A. Spontaneous fission half-lives for even nuclei with $Z \geq 92$. *Phys. Rev. C* 1976, **13**, 229–239.
67. Dvorak J., Bröchle W., Chelnokov M., Dressler R., Düllmann Ch. E., Eberhardt K., Gorshkov V., Jäger E., Krücken R., Kuznetsov A., Nagame Y., Nebel F., Novackova Z., Qin Z., Schädel M., Schausten B., Schimpf E., Semchenkov A., Thörle P., Türler A., Wegrzecki M., Wierczinski B., Yakushev A., Yerebin A. Doubly magic nucleus $^{270}_{108}\text{Hs}^{162}$. *Phys. Rev. Lett.* 2006, **97**, 242501.
68. Hofmann S., Ninov V., Heßberger F. P., Armbruster P., Folger H., Münzenberg G., Schött H. J., Popeko A. G., Yerebin A. V., Andreyev A. N., Saro S., Janik R., Leino M. Production and decay of $^{269}\text{110}$. *Z. Phys. A* 1995, **350**, 277–280.
69. Heßberger F. P., Münzenberg G., Armbruster P., Berthes G., Faust W., Hofmann S., Reisdorf W., Schmidt K. H., Ewald H., Güttner K. The recoil separator system at GSI - Description, experiments and further plans. *Lect. Notes Phys.* 1988, **317**, 289–296.
70. Heßberger F. P., Hofmann S., Ninov V., Armbruster P., Folger H., Münzenberg G., Schött H. J., Popeko A. G., Yerebin A. V., Andreyev A. N., Saro S. Spontaneous fission and alpha-decay properties of neutron deficient isotopes $^{257-253}\text{104}$ and $^{258}\text{106}$. *Z. Phys. A* 1997, **359**, 415–425.

71. Hofmann S. New elements - approaching $Z = 114$. *Rep. Prog. Phys.* 1998, 61, 639–689.
72. Hofmann S., Ninov V., Heßberger F. P., Armbruster P., Folger H., Münzenberg G., Schött H. J., Popeko A. G., Yeremin A. V., Andreyev A. N., Saro S., Janik R., Leino M. The new element 111. *Z. Phys. A* 1995, 350, 281–282.
73. Hofmann S., Ninov V., Heßberger F. P., Armbruster P., Folger H., Münzenberg G., Schött H. J., Popeko A. G., Yeremin A. V., Saro S., Janik R., Leino M. The new element 112. *Z. Phys. A* 1996, 354, 229–230.
74. Hofmann S., Heßberger F. P., Ackermann D., Münzenberg G., Antalic S., Cagarda P., Kindler B., Kojouharova J., Leino M., Lommel B., Mann R., Popeko A. G., Reshitko S., Saro S., Uusitalo J., Yeremin A. V. New results on elements 111 and 112. *Eur. Phys. J. A* 2002, 14, 147–157.
75. Hofmann S., Ackermann D., Antalic S., Burkhard H. G., Comas V. F., Dressler R., Gan Z., Heinz S., Heredia J. A., Heßberger F. P., Khuyagbaatar J., Kindler B., Kojouharov I., Kuusiniemi P., Leino M., Lommel B., Mann R., Münzenberg G., Nishio K., Popeko A. G., Saro S., Schött H. J., Streicher B., Sulignano B., Uusitalo J., Venhart M., Yeremin A. The reaction $^{48}\text{Ca} + ^{238}\text{U} \rightarrow ^{286}112^*$ studied at the GSI-SHIP. *Eur. Phys. J. A* 2007, 32, 251–260.
76. Düllmann Ch. E., Schädel M., Yakushev A., Türler A., Eberhardt K., Kratz J. V., Ackermann D., Andersson L.-L., Block M., Brüche W., Dvorak J., Essel H. G., Ellison P. A., Even J., Gates J. M., Gorshkov A., Graeger R., Gregorich K. E., Hartmann W., Herzberg R.-D., Heßberger F. P., Hild D., Hübner A., Jäger E., Khuyagbaatar J., Kindler B., Krier J., Kurz N., Lahiri S., Liebe D., Lommel B., Maiti M., Nitsche H., Omtvedt J. P., Parr E., Rudolph D., Runke J., Schausten B., Schimpf E., Semchenkov A., Steiner J., Thörle-Pospiech P., Uusitalo J., Wegrzecki M., Wiehl N. Production and decay of element 114: high cross sections and the new nucleus ^{277}Hs . *Phys. Rev. Lett.* 2010, 104, 252701.
77. Rudolph D., Forsberg U., Golubev P., Sarmiento L. G., Yakushev A., Andersson L.-L., Di Nitto A., Düllmann Ch. E., Gates J. M., Gregorich K. E., Gross C. J., Heßberger F. P., Herzberg R.-D., Khuyagbaatar J., Kratz J. V., Rykaczewski K., Schädel M., Åberg S., Ackermann D., Block M., Brand H., Carlsson B. G., Cox D., Derkx X., Eberhardt K., Even J., Fahlander C., Gerl J., Jäger E., Kindler B., Krier J., Kojouharov I., Kurz N., Lommel B., Mistry A., Mokry C., Nitsche H., Omtvedt J. P., Papadakis P., Ragnarsson I., Runke J., Schaffner H., Schausten B., Thörle-Pospiech P., Torres T., Traut T., Trautmann N., Türler A., Ward A., Ward D. E., Wiehl N. Spectroscopy of element 115 decay chains. *Phys. Rev. Lett.* 2013, 111, 112502.
78. Khuyagbaatar J., Yakushev A., Düllmann Ch. E., Ackermann D., Andersson L.-L., Asai M., Block M., Boll R. A., Brand H., Cox D. M., Dasgupta M., Derkx X., Di Nitto A., Eberhardt K., Even J., Evers M., Fahlander C., Forsberg U., Gates J. M., Gharibyan N., Golubev P., Gregorich K. E., Hamilton J. H., Hartmann W., Herzberg R.-D., Heßberger F. P., Hinde D. J., Hoffmann J., Hollinger R., Hübner A., Jäger E., Kindler B., Kratz J. V., Krier J., Kurz N., Laatiaoui M., Lahiri S., Lang R., Lommel B., Maiti M., Miernik K., Minami S., Mistry A., Mokry C., Nitsche H., Omtvedt J. P., Pang G. K., Papadakis P., Renisch D., Roberto J., Rudolph D., Runke J., Rykaczewski K. P., Sarmiento L. G., Schädel M., Schausten B., Semchenkov A., Shaughnessy D. A., Steinegger P., Steiner J., Tereshatov E. E., Thörle-Pospiech P., Tinschert K., Heidenreich T. T. D., Trautmann N., Türler A., Uusitalo J., Ward D. E., Wegrzecki M., Wiehl N., Cleve S. M. V., Yakusheva V. $^{48}\text{Ca} + ^{249}\text{Bk}$ fusion reaction leading to element $Z = 117$: long-lived α -decaying ^{270}Db and discovery of ^{266}Lr . *Phys. Rev. Lett.* 2014, 112, 172501.
79. Hofmann S., Heinz S., Mann R., Maurer J., Khuyagbaatar J., Ackermann D., Antalic S., Barth W., Block M., Burkhard H. G., Comas V. F., Dahl L., Eberhardt K., Gostic J., Henderson R. A., Heredia J. A., Heßberger F. P., Kenneally J. M., Kindler B., Kojouharov I., Kratz J. V., Lang R., Leino M., Lommel B., Moody K. J., Münzenberg G., Nelson S. L., Nishio K., Popeko A. G., Runke J., Saro S., Shaughnessy D. A., Stoyer M. A., Thörle-Pospiech P., Tinschert K., Trautmann N., Uusitalo J., Wilk P. A., Yeremin A. V. The reaction $^{48}\text{Ca} + ^{248}\text{Cm} \rightarrow ^{296}116^*$ studied at the GSI-SHIP. *Eur. Phys. J. A* 2012, 48, 62.
80. Oganessian Y. T., Utyonkov V. K., Lobanov Y. V., Abdullin F. S., Polyakov A. N., Sagaidak R. N., Shirokovsky I. V., Tsyganov Y. S., Voinov A. A., Mezentshev A. N., Subbotin V. G., Sukhov A. M., Subotic K., Zagrebaev V. I., Dmitriev S. N., Henderson R. A., Moody K. J., Kenneally J. M., Landrum J. H., Shaughnessy D. A., Stoyer M. A., Stoyer N. J., Wilk P. A. Attempt to produce element 120 in the $^{244}\text{Pu} + ^{58}\text{Fe}$ reaction. *Phys. Rev. C* 2009, 79, 024603.
81. Hofmann S., Ackermann D., Antalic S., Comas V. F., Heinz S., Heredia J. A., Heßberger F. P., Khuyagbaatar J., Kindler B., Kojouharov I., Leino M., Lommel B., Mann R., Nishio K., Popeko A. G., Saro S., Uusitalo J., Venhart M., Yeremin A. V. *Probing Shell Effects at $Z=120$ and $N=184$* , GSI Scientific Report 2008 (GSI Report 2009-1); GSI: Darmstadt, 2009.
82. Hofmann S., Heinz S., Mann R., Maurer J., Münzenberg G., Antalic S., Barth W., Burkhard H. G., Dahl L., Eberhardt K., Grzywacz R., Hamilton J. H., Henderson R. A., Kenneally J. M., Kindler B., Kojouharov I., Lang R., Lommel B., Miernik K., Miller D., Moody K. J., Morita K., Nishio K., Popeko A. G., Roberto J. B., Runke J., Rykaczewski K. P., Saro S., Scheidenberger C., Schött H. J., Shaughnessy D. A., Stoyer M. A., Thörle-Pospiech P., Tinschert K., Trautmann N., Uusitalo J., Yeremin A. V. Review of even element super-heavy nuclei and search for element 120. *Eur. Phys. J. A* 2016, 52, 180.
83. Heßberger F. P., Ackermann D. Some critical remarks on a sequence of events interpreted to possibly originate from a decay chain of an element 120 isotope. *Eur. Phys. J. A* 2017, 53, 123.
84. Albers H. M., Khuyagbaatar J., Hinde D. J., Carter I. P., Cook K. J., Dasgupta M., Düllmann Ch. E., Eberhardt K., Jeung D. Y., Kalkal S., Kindler B., Lobanov N. R., Lommel B., Mokry C., Prasad E., Rafferty D. C., Runke J., Sekizawa K., Sengupta C., Simenel C., Simpson E. C., Smith J. F., Thörle-Pospiech P., Trautmann N., Vo-Phuoc K., Walshe J., Williams E., Yakushev A. Zeptosecond contact times for element $Z = 120$ synthesis. *Phys. Lett. B* 2020, 808, 135626.
85. Düllmann Ch. E., Yakushev A., Khuyagbaatar J., Rudolph D., Nitsche H., Ackermann D., Andersson L.-L., Badura E., Block M., Brand H., Cox D. M., Eberhardt K., Ellison P. A., Esker N. E., Even J., Fahlander C., Forsberg U., Gates J. M., Gregorich K. E., Golubev P., Gothe O., Hartmann W., Herzberg R.-D., Heßberger F. P., Hoffmann J., Hollinger R., Hübner A., Jäger E., Jeppsson J., Kindler B., Klein S., Kojouharov I., Kratz J. V., Krier J., Kurz N., Lahiri S., Lommel B., Maiti M., Mändl R., Merchan E., Minami S., Mistry A., Mokry C., Omtvedt J. P., Pang G. K., Pysmenetska I., Renisch D., Runke J., Sarmiento L. G.,

- Schädel M., Schaffner H., Schausten B., Semchenkov A., Steiner J., Thörle-Pospiech P., Trautmann N., Türler A., Uusitalo J., Ward D., Wiczorek P., Wiehl N., Wegrzecki M., Yakusheva V. *Study of the $^{50}\text{Ti} + ^{249}\text{Cf}$ fusion-evaporation Reaction Leading to Element 120 at the Gas-Filled Recoil Separator TASCA*. (to be published).
86. Khuyagbaatar J., Yakushev A., Düllmann Ch. E., Ackermann D., Andersson L.-L., Asai M., Block M., Boll R. A., Brand H., Cox D. M., Dasgupta M., Derkx X., Di Nitto A., Eberhardt K., Even J., Evers M., Fahlander C., Forsberg U., Gates J. M., Gharibyan N., Golubev P., Gregorich K. E., Hamilton J. H., Hartmann W., Herzberg R.-D., Heßberger F. P., Hinde D. J., Hoffmann J., Hollinger R., Hübner A., Jäger E., Kindler B., Kratz J. V., Krier J., Kurz N., Laatiaoui M., Lahiri S., Lang R., Lommel B., Maiti M., Miernik K., Minami S., Mistry A. K., Mokry C., Nitsche H., Omtvedt J. P., Pang G. K., Papadakis P., Renisch D., Roberto J. B., Rudolph D., Runke J., Rykaczewski K. P., Sarmiento L. G., Schädel M., Schausten B., Semchenkov A., Shaughnessy D. A., Steinegger P., Steiner J., Tereshatov E. E., Thörle-Pospiech P., Tinschert K., Torres De Heidenreich T., Trautmann N., Türler A., Uusitalo J., Wegrzecki M., Wiehl N., Cleve S. M. V., Yakusheva V. Search for elements 119 and 120. *Phys. Rev. C* 2020, *102*, 064602.
 87. Schädel M. Chemistry of superheavy elements. *Radiochim. Acta* 2012, *100*, 579–604.
 88. Pershina V. Theoretical chemistry of the heaviest elements. In *The Chemistry of Superheavy Elements*; Schädel M., Shaughnessy D., Eds.; Springer: Heidelberg, 2014, pp. 135–239.
 89. Kratz J. V. Nuclear and Radiochemistry – Fundamentals and Applications, 4th ed., *Chapter 17 Radioelements*; Wiley VCH: Weinheim, Germany, 2021; pp 609–734.
 90. Schädel M., Bröchle W., Jäger E., Schimpf E., Kratz J. V., Scherer U. W., Zimmermann H. P. ARCA II - a new apparatus for fast, repetitive HPLC separations. *Radiochim. Acta* 1989, *48*, 171–176.
 91. Kratz J. V., Zimmerman H. P., Scherer U. W., Schädel M., Bröchle W., Gregorich K. E., Gannett C. M., Hall H. L., Henderson C. M., Lee D. M., Leyba J. D., Nurmia M., Hoffman D. C., Gäggeler H., Jost D., Baltensperger U., Nai-Qi Y., Türler A., Lienert C. Chemical properties of element 105 in aqueous solution: halide complex formation and anion exchange into triisooctyl amine. *Radiochim. Acta* 1989, *48*, 121–133.
 92. Kratz J. V., Guber M. K., Zimmermann H. P., Schädel M., Bröchle W., Schimpf E., Gregorich K. E., Türler A., Hannink N. J., Czerwinski K. R., Kadkhodayan B., Lee D. M., Nurmia M. J., Hoffman D. C., Gäggeler H., Jost D., Kovacs J., Scherer U. W., Weber A. New nuclide ^{263}Ha . *Phys. Rev. C* 1992, *45*, 1064–1069.
 93. Johnson E., Pershina V., Fricke B. Ionization potentials of seaborgium. *J. Phys. Chem.* 1999, *103*, 8458–8462.
 94. Pershina V., Fricke B. Group 6 dioxidichlorides MO_2Cl_2 (M = Cr, Mo, W, and element 106, Sg): the electronic structure and thermochemical stability. *J. Phys. Chem.* 1996, *100*, 8748–8751.
 95. Pershina V., Kratz J. V. Solution chemistry of element 106: theoretical predictions of hydrolysis of group 6 cations Mo, W, and Sg. *Inorg. Chem.* 2001, *40*, 776–780.
 96. Türler A. Gas phase chemistry experiments with transactinide elements. *Radiochim. Acta* 1996, *72*, 7–17.
 97. Schädel M., Bröchle W., Dressler R., Eichler B., Gäggeler H. W., Günther R., Gregorich K. E., Hoffman D. C., Hübener S., Jost D. T., Kratz J. V., Paulus W., Schumann D., Timokhin S., Trautmann N., Türler A. Chemical properties of element 106 (seaborgium). *Nature* 1997, *388*, 55–57.
 98. Schädel M., Bröchle W., Schausten B., Schimpf E., Jäger E., Wirth G., Günther R., Kratz J. V., Paulus W., Seibert A., Thörle P., Trautmann N., Zauner S., Schumann D., Andrassy M., Misiak R., Gregorich K. E., Hoffman D. C., Lee D. M., Sylwester E. R., Nagame Y., Oura Y. First aqueous chemistry with seaborgium (element 106). *Radiochim. Acta* 1997, *77*, 149–159.
 99. Schädel M., Bröchle W., Jäger E., Schausten B., Wirth G., Paulus W., Günther R., Eberhardt K., Kratz J. V., Seibert A., Strub E., Thörle P., Trautmann N., Waldek A., Zauner S., Schumann D., Kirbach U., Kubica B., Misiak R., Nagame Y., Gregorich K. E. Aqueous chemistry of seaborgium (Z = 106). *Radiochim. Acta* 1998, *83*, 163–165.
 100. Türler A., Bröchle W., Dressler R., Eichler B., Eichler R., Gäggeler H. W., Gärtner M., Glatz J.-P., Gregorich K. E., Hübener S., Jost D. T., Lebedev V. Y., Pershina V. G., Schädel M., Taut S., Timokhin S. N., Trautmann N., Vahle A., Yakushev A. B. First measurement of a thermochemical property of a seaborgium compound. *Angew. Chem. Int. Ed.* 1999, *38*, 2212–2213.
 101. Hübener S., Taut S., Vahle A., Dressler R., Eichler B., Gäggeler H. W., Jost D. T., Piguet D., Türler A., Bröchle W., Jäger E., Schädel M., Schimpf E., Kirbach U., Trautmann N., Yakushev A. B. Physico-chemical characterization of seaborgium as oxide hydroxide. *Radiochim. Acta* 2001, *89*, 737–741.
 102. Türler A., Dressler R., Eichler B., Gäggeler H. W., Jost D. T., Schädel M., Bröchle W., Gregorich K. E., Trautmann N., Taut S. Decay properties of $^{265}\text{Sg}(Z=106)$ and $^{266}\text{Sg}(Z=106)$. *Phys. Rev. C* 1998, *57*, 1648.
 103. Eichler R., Eichler B. Thermochemical data from gas-phase adsorption and methods of their estimation. In *The Chemistry of Superheavy Elements*; Schädel M., Shaughnessy D., Eds.; Springer: Heidelberg, 2014; pp. 375–413.
 104. Düllmann Ch. E., Türler A. $^{248}\text{Cm}(^{22}\text{Ne},\text{xn})^{270-x}\text{Sg}$ reaction and the decay properties of ^{265}Sg reexamined. *Phys. Rev. C* 2008, *77*, 064320.
 105. Haba H., Kaji D., Kudou Y., Morimoto K., Morita K., Ozeki K., Sakai R., Sumita T., Yoneda A., Kasamatsu Y., Komori Y., Shinohara A., Kikunga H., Kudo H., Nishio K., Ooe K., Sato N., Tsukada K. Production of ^{265}Sg in the $^{248}\text{Cm}(^{22}\text{Ne},5\text{n})^{265}\text{Sg}$ reaction and decay properties of two isomeric states in ^{265}Sg . *Phys. Rev. C* 2012, *85*, 024611.
 106. Dvorak J., Bröchle W., Chelnokov M., Dressler R., Düllmann Ch. E., Dvorakova Z., Eberhardt K., Jäger E., Krücken R., Kuznetsov A., Nagame Y., Nebel F., Nishio K., Perego R., Qin Z., Schädel M., Schausten B., Schimpf E., Schuber R., Semchenkov A., Thörle P., Türler A., Wegrzecki M., Wierczinski B., Yakushev A., Yerebin A. Observation of the $3n$ evaporation channel in the complete hot-fusion reaction $^{26}\text{Mg} + ^{248}\text{Cm}$ leading to the new superheavy nuclide ^{271}Hs . *Phys. Rev. Lett.* 2008, *100*, 132503.
 107. Even J., Yakushev A., Düllmann Ch. E., Dvorak J., Eichler R., Gothe O., Hild D., Jäger E., Khuyagbaatar J., Kratz J. V., Krier J., Niewisch L., Nitsche H., Pysmenetska I., Schädel M., Schausten B., Türler A., Wiehl N., Wittwer D. Rapid synthesis of radioactive transition-metal carbonyl complexes at ambient conditions. *Inorg. Chem.* 2012, *51*, 6431–6433.

108. Eberhardt K., Geppert C. The research reactor TRIGA Mainz – a strong and versatile neutron source for science and education. *Radiochim. Acta* 2019, *107*, 535–546.
109. Even J., Yakushev A., Düllmann Ch. E., Haba H., Asai M., Sato T. K., Brand H., Di Nitto A., Eichler R., Fan F. L., Hartmann W., Huang M., Jäger E., Kaji D., Kanaya J., Kaneya Y., Khuyagbaatar J., Kindler B., Kratz J. V., Krier J., Kudou Y., Kurz N., Lommel B., Miyashita S., Morimoto K., Morita K., Murakami M., Nagame Y., Nitsche H., Ooe K., Qin Z., Schädel M., Steiner J., Sumita T., Takeyama M., Tanaka K., Toyoshima A., Tsukada K., Türler A., Usoltsev I., Wakabayashi Y., Wang Y., Wiehl N., Yamaki S. Synthesis and detection of a seaborgium carbonyl complex. *Science* 2014, *345*, 1491–1493.
110. Ilias M., Pershina V. Hexacarbonyls of Mo, W, and Sg: metal–CO bonding revisited. *Inorg. Chem.* 2017, *56*, 1638–1645.
111. Düllmann Ch. E., Bröchle W., Dressler R., Eberhardt K., Eichler B., Eichler R., Gäggeler H. W., Ginter T. N., Glaus F., Gregorich K. E., Hoffman D. C., Jäger E., Jost D. T., Kirbach U. W., Lee D. M., Nitsche H., Patin J. B., Pershina V., Piguet D., Qin Z., Schädel M., Schausten B., Schimpf E., Schött H. J., Soverna S., Sudowe R., Thörle P., Timokhin S. N., Trautmann N., Türler A., Vahle A., Wirth G., Yakushev A. B., Zielinski P. M. Chemical investigation of hassium (element 108). *Nature* 2002, *418*, 859–862.
112. Türler A. Nuclear structure and reaction studies near doubly magic ^{270}Hs . *Radiochim. Acta* 2012, *100*, 75–83.
113. Düllmann Ch. E., Eichler B., Eichler R., Gäggeler H. W., Jost D. T., Piguet D., Türler A. IVO, a device for in situ Volatilization and On-line detection of products from heavy ion reactions. *Nucl. Instrum. Methods Phys. Res. A* 2002, *479*, 631–639.
114. Kirbach U. W., Folden C. M. III, Ginter T. N., Gregorich K. E., Lee D. M., Ninov V., Omtvedt J. P., Patin J. B., Seward N. K., Strellis D. A. The Cryo-Thermochromatographic Separator (CTS): a new rapid separation and α -detection system for on-line chemical studies of highly volatile osmium and hassium ($Z=108$) tetroxides. *Nucl. Instrum. Methods A* 2002, *484*, 587–594.
115. Pershina V., Anton J., Jacob T. Fully relativistic density-functional-theory calculations of the electronic structures of MO_4 ($M = \text{Ru}, \text{Os}$, and element 108, Hs) and prediction of physisorption. *Phys. Rev. A* 2008, *78*, 032518.
116. von Zweidorf A., Angert R., Bröchle W., Bürger S., Eberhardt K., Eichler R., Hummrich H., Jäger E., Kling H.-O., Kratz J. V., Kuczewski B., Langrock G., Mendel M., Rieth U., Schädel M., Schausten B., Schimpf E., Thörle P., Trautmann N., Tsukada K., Wiehl N., Wirth G. Evidence for the formation of sodium hassate(VIII). *Radiochim. Acta* 2004, *92*, 855–861.
117. Oganessian Y. T., Utyonkov V. K., Abdullin F. S., Dmitriev S. N., Graeger R., Henderson R. A., Itkis M. G., Lobanov Y. V., Mezentsev A. N., Moody K. J., Nelson S. L., Polyakov A. N., Ryabinin M. A., Sagaidak R. N., Shaughnessy D. A., Shirokovsky I. V., Stoyer M. A., Stoyer N. J., Subbotin V. G., Subotic K., Sukhov A. M., Tsyganov Y. S., Türler A., Voinov A. A., Vostokin G. K., Wilk P. A., Yakushev A. Synthesis and study of decay properties of the doubly magic nucleus ^{270}Hs in the $^{226}\text{Ra} + ^{48}\text{Ca}$ reaction. *Phys. Rev. C* 2013, *87*, 034605.
118. Eichler R., Bröchle W., Buda R., Bürger S., Dressler R., Düllmann Ch. E., Dvorak J., Eberhardt K., Eichler B., Folden C. M. III, Gäggeler H. W., Gregorich K. E., Haenssler F., Hoffman D. C., Hummrich H., Jäger E., Schimpf E., Semchenov A., Soverna S., Sudowe R., Trautmann N., Thörle P., Türler A., Wierczinski B., Wiehl N., Wilk P. A., Wirth G., Yakushev A., von Zweidorf A. Attempts to chemically investigate element 112. *Radiochim. Acta* 2006, *94*, 181–191.
119. Yakushev A., Eichler R. Gas-phase chemistry of element 114, flerovium. *EPJ Web Conf.* 2016, *131*, 07003.
120. Eichler B. Das Flüchtigkeitsverhalten von Transactiniden im Bereich um $Z = 114$ (Voraussage). *Kernenergie* 1976, *19*, 307–311.
121. Pitzer K. S. Are elements 112, 114, and 118 relatively inert gases? *J. Chem. Phys.* 1975, *63*, 1032–1033.
122. Pershina V. A relativistic periodic DFT study on interaction of superheavy elements 112 (Cn) and 114 (Fl) and their homologs Hg and Pb, respectively, with a quartz surface. *Phys. Chem. Chem. Phys.* 2016, *18*, 17750–17756.
123. Pershina V. Reactivity of superheavy elements Cn, Nh, and Fl and their lighter homologues Hg, Tl, and Pb, respectively, with a gold surface from periodic DFT calculations. *Inorg. Chem.* 2018, *57*, 3948–3955.
124. Trombach L., Ehler S., Grimme S., Schwerdtfeger P., Mewes J.-M. Exploring the chemical nature of super-heavy main-group elements by means of efficient plane-wave density-functional theory. *Phys. Chem. Chem. Phys.* 2016, *21*, 18048–18058.
125. Pershina V., Ilias M., Yakushev A. Reactivity of the superheavy element 115, Mc, and its lighter homologue, Bi, with respect to gold and hydroxylated quartz surfaces from periodic relativistic DFT calculations: a comparison with element 113, Nh. *Inorg. Chem.* 2021, *60*, 9796–9804.
126. Eichler R., Aksenov N. V., Belozero A. V., Bozhikov G. A., Chepigin V. I., Dmitriev S. N., Dressler R., Gäggeler H. W., Gorshkov V. A., Haenssler F., Itkis M. G., Laube A., Lebedev V. Y., Malyshev O. N., Oganessian Y. T., Petrushkin O. V., Piguet D., Rasmussen P., Shishkin S. V., Shutov A. V., Svirikhin A. I., Tereshatov E. E., Vostokin G. K., Wegrzecki M., Yeregin A. Chemical characterization of element 112. *Nature* 2007, *447*, 72–75.
127. Dmitriev S. N., Aksenov N. V., Albin Y. V., Bozhikov G. A., Chelnokov M. L., Chepygin V. I., Eichler R., Isaev A. V., Katrasev D. E., Lebedev V. Y., Malyshev O. N., Petrushkin O. V., Porobanuk L. S., Ryabinin M. A., Sabel'nikov A. V., Sokol E. A., Svirikhin A. V., Starodub G. Y., Usoltsev I., Vostokina G. K., Yeregin A. V. Pioneering experiments on the chemical properties of element 113. *Mendeleev Commun.* 2014, *24*, 253–256.
128. Eichler R., Aksenov N. V., Albin Y. V., Belozero A. V., Bozhikov G. A., Chepigin V. I., Dmitriev S. N., Dressler R., Gäggeler H. W., Gorshkov V. A., Henderson R. A., Johnsen A. M., Kenneally J. M., Lebedev V. Y., Malyshev O. N., Moody K. J., Oganessian Y. T., Petrushkin O. V., Piguet D., Popeko A. G., Rasmussen P., Serov A. A., Shaughnessy D. A., Shishkin S. V., Shutov A. V., Stoyer M. A., Stoyer N. J., Svirikhin A. I., Tereshatov E. E., Vostokin G. K., Wegrzecki M., Wilk P. A., Wittwer D., Yeregin A. V. Indication for a volatile element 114. *Radiochim. Acta* 2010, *98*, 133–139.
129. Yakushev A., Gates J. M., Türler A., Schädel M., Düllmann Ch. E., Ackermann D., Andersson L.-L., Block M., Bröchle W., Dvorak J., Eberhardt K., Essel H. G., Even J., Forsberg U., Gorshkov A., Graeger R., Gregorich K. E., Hartmann W., Herzberg R.-D., Heßberger F. P., Hild D., Hübner A., Jäger E., Khuyagbaatar J., Kindler B., Kratz J. V., Krier J., Kurz N., Lommel B., Niewisch L. J., Nitsche H., Omtvedt J. P., Parr E., Qin Z., Rudolph D., Runke J., Schausten B., Schimpf E., Semchenov A., Steiner J., Thörle-Pospiech P., Uusitalo J., Wegrzecki M., Wiehl N. Superheavy

- element flerovium (element 114) is a volatile metal. *Inorg. Chem.* 2014, 53, 1624–1629.
130. Yakushev A., Lens L., Düllmann Ch. E., Khuyagbaatar J., Di Nitto A., Jäger E., Krier J., Runke J., Albers H. M., Asai M., Block M., Brand H., Despotopulos J., Eberhardt K., Forsberg U., Golubev P., Götz M., Götz S., Haba H., Harkness-Brennan L., Herzberg R.-D., Hinde D., Hübner A., Jourdan M., Judson D., Kindler B., Komori Y., Konki J., Kratz J. V., Kurz N., Laatiaoui M., Lahiri S., Lommel B., Maiti M., Mistry A. K., Mokry C., Moody K. J., Nagame Y., Omtvedt J. P., Papadakis P., Pershina V., Rudolph D., Sarmiento L. G., Sato T. K., Schädel M., Scharrer P., Schausten B., Shaughnessy D. A., Steiner J., Thörle-Pospiech P., Toyoshima A., Trautmann N., Tsukada K., Uusitalo J., Voss K.-O., Ward A., Wegrzecki M., Wiehl N., Williams E., Yakusheva V. On the reactivity of element 114, flerovium. *Phys. Chem. Chem. Phys.* 2021. (submitted).
 131. Düllmann Ch. E., Folden C. M. III, Gregorich K. E., Hoffman D. C., Leitner D., Pang G. K., Sudowe R., Zielinski P. M., Nitsche H. Heavy-ion-induced production and physical pre-separation of short-lived isotopes for chemistry experiments. *Nucl. Instrum. Methods Phys. Res. A* 2005, 551, 528–539.
 132. Yakushev A., Lens L., Düllmann Ch. E., Block M., Brand H., Calverley T., Dasgupta M., Di Nitto A., Götz M., Götz S., Haba H., Harkness-Brennan L., Herzberg R.-D., Heßberger F. P., Hinde D., Hübner A., Jäger E., Judson D., Khuyagbaatar J., Kindler B., Komori Y., Konki J., Kratz J. V., Krier J., Kurz N., Laatiaoui M., Lommel B., Lorenz C., Maiti M., Mistry A. K., Mokry C., Nagame Y., Papadakis P., Sâmark-Roth A., Rudolph D., Runke J., Sarmiento L. G., Sato T. K., Schädel M., Scharrer P., Schausten B., Steiner J., Thörle-Pospiech P., Toyoshima A., Trautmann N., Uusitalo J., Ward A., Wegrzecki M., Yakusheva V. First study on nihonium (Nh, element 113) chemistry at TASCA. *Front. Chem.* 2021, 9, 753738.
 133. Aksenov N. V., Steinegger P., Abdullin F. S., Albin Y. V., Bozhikov G. A., Chepigina V. I., Eichler R., Lebedev V. Y., Madumarov A. S., Malyshev O. N., Petrushkin O. V., Polyakov A. N., Popov Y. A., Sabel'nikov A. V., Sagaidak R. N., Shirokovsky I. V., Shumeiko M. V., Starodub G. Y., Tsyganov Y. S., Utyonkov V. K., Voinov A. A., Vostokin G. K., Yereimin A. V., Dmitriev S. N. On the volatility of nihonium (Nh, Z = 113). *Eur. Phys. J. A* 2017, 53, 158.
 134. Dmitriev S. N., Popeko A. G. High-power radioactive targets as one of the key problems in further development of the research program on synthesis of new superheavy elements. *J. Radioanal. Nucl. Chem.* 2015, 305, 927–933.
 135. Lommel B., Gembalies-Datz D., Hartmann W., Hofmann S., Kindler B., Klemm J., Kojouharova J., Steiner J. Improvement of the target durability for heavy-element production. *Nucl. Instrum. Methods Phys. Res. A* 2002, 480, 16–21.
 136. Kindler B., Ackermann D., Hartmann W., Hessberger F. P., Hofmann S., Lommel B., Mann R., Steiner J. Chemical compound targets for SHIP on heated carbon backings. *Nucl. Instrum. Methods Phys. Res. A* 2006, 561, 107–111.
 137. Kindler B., Ackermann D., Hartmann W., Hessberger F. P., Hofmann S., Hübner A., Lommel B., Mann R., Steiner J. Uranium fluoride and metallic uranium as target materials for heavy-element experiments at SHIP. *Nucl. Instrum. Methods Phys. Res. A* 2008, 590, 126–130.
 138. Lommel B., Celik Ayik E., Hübner A., Kindler B., Steiner J., Yakusheva V. Uranium targets for heavy-ion accelerators. *EPJ Web Conf.* 2020, 229, 03006.
 139. Lommel B., Hartmann W., Kindler B., Klemm J., Steiner J. Preparation of self-supporting carbon thin films. *Nucl. Instrum. Methods Phys. Res. A* 2002, 480, 199–203.
 140. Lommel B., Bröchle W., Eberhardt K., Hartmann W., Hübner A., Kindler B., Kratz J. V., Liebe D., Schädel M., Steiner J. Backings and targets for chemical and nuclear studies of transactinides with TASCA. *Nucl. Instrum. Methods Phys. Res. A* 2008, 590, 141–144.
 141. Parker W., Falk R. Molecular plating: a method for the electrolytic formation of thin inorganic films. *Nucl. Instrum. Methods* 1962, 16, 355–357.
 142. Trautmann N., Folger H. Preparation of actinide targets by electrodeposition. *Nucl. Instrum. Methods Phys. Res.* 1989, A282, 102–106.
 143. Eberhardt K., Bröchle W., Düllmann Ch. E., Gregorich K. E., Hartmann W., Hübner A., Jäger E., Kindler B., Kratz J. V., Liebe D., Lommel B., Maier H.-J., Schädel M., Schausten B., Schimpf E., Semchenkov A., Steiner J., Szerypo J., Thörle P., Türlér A., Yakushev A. Preparation of targets for the gas-filled recoil separator TASCA by electrochemical deposition and design of the TASCA target wheel assembly. *Nucl. Instrum. Methods Phys. Res. A* 2008, 590, 134–140.
 144. Runke J., Düllmann Ch. E., Eberhardt K., Ellison P. A., Gregorich K. E., Hofmann S., Jäger E., Kindler B., Kratz J. V., Krier J., Lommel B., Mokry C., Nitsche H., Roberto J. B., Rykaczewski K. P., Schädel M., Thörle-Pospiech P., Trautmann N., Yakushev A. Preparation of actinide targets for the synthesis of the heaviest elements. *J. Radioanal. Nucl. Chem.* 2014, 299, 1081–1084.
 145. Vascon A., Santi S., Isse A. A., Reich T., Drebert J., Christ H., Düllmann Ch. E., Eberhardt K. Elucidation of constant current density molecular plating. *Nucl. Instrum. Methods Phys. Res. A* 2012, 696, 180–191.
 146. Meyer C.-C., Dragoun A., Düllmann Ch. E., Haas R., Jäger E., Kindler B., Lommel B., Prosvetov A., Rapps M., Renisch D., Simon P., Tomut M., Trautmann C., Yakushev A. Chemical conversions in lead thin films induced by heavy-ion beams at Coulomb barrier energies. *Nucl. Instrum. Methods Phys. Res. A* 2021, 1028, 166365.
 147. Araújo Melo D. M., Vicentini G., Zinner L. B., De Simone C. A., Castellano E. E. Synthesis, properties and structure of hexaquo-tris(N,N-dimethylformamide)-lanthanide trifluoromethanesulfonates. *Inorg. Chim. Acta.* 1988, 146, 123–127.
 148. Yang Q., Liu P., Yang Y., Tong Y. Study on electroreduction of Eu(III) and electrodeposition of Eu–Co in europium toluenesulfonate + DMF. *J. Electroanal. Chem.* 1998, 456, 223–227.
 149. Schumacher P. D., Doyle J. L., Schenk J. O., Clark S. B. Electroanalytical chemistry of lanthanides and actinides. *Rev. Anal. Chem.* 2013, 32, 159–171.
 150. Miski-Oglu M., Aulenbacher K., Barth W., Basten M., Burandt C., Busch M., Conrad T., Dziuba F., Gettmann V., Heilmann M., Kuerzeder T., List J., Lauber S., Podlech H., Rubin A., Schnase A., Schwarz M., Yaramyshev S. Progress in SRF CH-cavities for the HELIAC cw linac at GSI. In *Proc. 19th Int. Conf. on RF Superconductivity*, Dresden, Germany, June 30 - July 05, 2019.
 151. Khuyagbaatar J., Albers H. M., Block M., Brand H., Cantemir R. A., Di Nitto A., Düllmann Ch. E., Götz M., Götz S., Heßberger F. P., Jäger E., Kindler B., Kratz J. V., Krier J., Kurz N., Lommel B.,

- Lens L., Mistry A., Schausten B., Uusitalo J., Yakushev A. Search for electron-capture delayed fission in the new isotope ^{244}Md . *Phys. Rev. Lett.* 2020, *125*, 142504.
152. Khuyagbaatar J., Brand H., Cantemir R. A., Düllmann Ch. E., Götz M., Götz S., Heßberger F. P., Jäger E., Kindler B., Krier J., Kurz N., Lommel B., Schausten B., Yakushev A. Isomeric states in ^{256}Rf . *Phys. Rev. C* 2021, *103*, 064303.
153. Sămark-Roth A., Cox D. M., Eberth J., Golubev P., Rudolph D., Sarmiento L. G., Tocabens G., Ginsz M., Pirard B., Compex Quirin. P. A cubic germanium detector. *Eur. Phys. J. A* 2020, *56*, 141.
154. Sămark-Roth A., Cox D. M., Rudolph D., Sarmiento L. G., Carlsson B. G., Egido J. L., Golubev P., Heery J., Yakushev A., Åberg S., Albers H. M., Albertsson M., Block M., Brand H., Calverley T., Cantemir R., Clark R. M., Düllmann Ch. E., Eberth J., Fahlander C., Forsberg U., Gates J. M., Giacoppo F., Götz M., Götz S., Herzberg R.-D., Hrabar Y., Jäger E., Judson D., Khuyagbaatar J., Kindler B., Kojouharov I., Kratz J. V., Krier J., Kurz N., Lens L., Ljungberg J., Lommel B., Louko J., Meyer C.-C., Mistry A., Mokry C., Papadakis P., Parr E., Pore J. L., Ragnarsson I., Runke J., Schädel M., Schaffner H., Schausten B., Shaughnessy D. A., Thörle-Pospiech P., Trautmann N., Uusitalo J. Spectroscopy along flerovium decay chains: discovery of ^{280}Ds and an excited state in ^{282}Cn . *Phys. Rev. Lett.* 2021, *126*, 032503.
155. Andersson L.-L., Rudolph D., Golubev P., Herzberg R.-D., Hoischen R., Merchán E., Ackermann D., Düllmann Ch. E., Eberhardt K., Even J., Gerl J., Heßberger F. P., Jäger E., Khuyagbaatar J., Kojouharov I., Kratz J. V., Krier J., Kurz N., Prokopowicz W., Schädel M., Schaffner H., Schausten B., Schimpf E., Semchenkov A., Türler A., Wollersheim H.-J., Yakushev A., Thörle-Pospiech P., Hartmann W., Hübner A., Lommel B., Kindler B., Steiner J. TASISpec - A highly efficient multi-coincidence spectrometer for nuclear structure investigations of the heaviest nuclei. *Nucl. Instrum. Meth. Phys. Res. A* 2010, *622*, 164–170.
156. Varentsov V., Yakushev A. Concept of a new universal high-density gas stopping cell setup for study of gas-phase chemistry and nuclear properties of super heavy elements (UniCell). *Nucl. Instrum. Methods Phys. Res. A* 2019, *940*, 206–214.
157. Block M. Direct mass measurements and ionization potential measurements of the actinides. *Radiochim. Acta* 2019, *107*, 821–831.